AIP Advances

# Acoustic cavitation model based on a novel reduced order gas pressure law

Cite as: AIP Advances **11**, 115309 (2021); https://doi.org/10.1063/5.0068152
Submitted: 23 August 2021 • Accepted: 04 October 2021 • Published Online: 03 November 2021

Can F. Delale and Şenay Pasinlioğlu

# Acoustic cavitation model based on a novel reduced order gas pressure law

Cite as: AIP Advances 11, 115309 (2021); doi: 10.1063/5.0068152
Submitted: 23 August 2021 • Accepted: 4 October 2021 •
Published Online: 3 November 2021



Can F. Delale[1,a] and Şenay Pasinlioğlu[2,b]

## AFFILIATIONS

[1] Department of Mechanical Engineering, MEF University, Ayazaga Cad. No. 4, 34396 Maslak, Sariyer, Istanbul, Turkey
[2] Department of Mathematics, Istanbul Technical University, Ayazaga Campus, 34469 Maslak, Istanbul, Turkey

[a] Author to whom correspondence should be addressed: delalec@mef.edu.tr
[b] pasinliogl@itu.edu.tr

## ABSTRACT

The thermal behavior of a spherical gas bubble in a liquid excited by an acoustic pressure signal is investigated by constructing an iterative solution of the energy balance equations between the gas bubble and the surrounding liquid in the uniform pressure approximation. This iterative solution leads to hierarchy equations for the radial partial derivatives of the temperature at the bubble wall, which control the temporal rate of change of the gas pressure and gas temperature within the bubble. In particular, a closure relation for the hierarchy equations is introduced based on the ansatz that approximates the rapid change of state during the collapse of the bubble from almost isothermal to almost adiabatic behavior by time averaging the complex dynamics of change of state over a relatively short characteristic time. This, in turn, leads to the desired reduced order gas pressure law exhibiting power law dependence on the bubble wall temperature and on the bubble radius, with the polytropic index depending on the isentropic exponent of the gas and on a parameter that is a function of the Péclet number and a characteristic time scale. Results of the linear theory for gas bubbles are recovered by identifying this parameter as a function of the Péclet number based on the Minnaert frequency. The novel gas pressure law is then validated against the near-isothermal solution and against the results of the numerical simulations of the original energy balance equations for large amplitude oscillations using spectral methods. Consequently, an acoustic cavitation model that accounts for phase change but that neglects mass diffusion is constructed by employing the reduced order gas pressure law together with the Plesset–Zwick solution for the bubble wall temperature and the Keller–Miksis equation for spherical bubble dynamics. Results obtained using variable interface properties for acoustically driven cavitation bubbles in water show that the time variations of the bubble radius and the bubble wall temperature lie between those obtained by the isothermal and adiabatic laws depending on the value of the Péclet number and the characteristic time scale.



## I. INTRODUCTION

In nonlinear bubble dynamics, the thermal behavior of bubbles during the final stage of collapse, where the pressure and temperature within the bubble can reach extremely high values, has received considerable interest because of its wide range of applications in cavitation,[1–3] sonochemistry,[4] single-bubble sonoluminescence,[5,6] and medical ultrasound.[7,8] In this case, the equations of motion describing the dynamics of spherical gas or gas/vapor bubbles are very complex, involving the solution of partial differential equations for the conservation of mass and energy together with momentum balance in both the gaseous and the liquid phases linked by interface conditions and equations of phase change. Although full numerical computations of these equations are available for single bubbles,[9,10] the complexity and accuracy of the numerical solutions require the need for simplified equations and expressions. Early attempts of modifying the adiabatic approximation for the gas pressure in spherical bubble dynamics by artificially increasing the liquid viscosity were not found satisfactory since the thermal damping affecting the nonlinear oscillations was overestimated in comparison with experiments.[11] Various models that address the effect of the thermal behavior of the bubble on the

gas pressure inside the bubble have been constructed,[12–16] but either they are still too complex to be easily and efficiently implemented for a variety of applications or they rely on assumptions and approximations that need to be verified. Recently, these models and their extensions have also been compared with the results of numerical simulations in various applications.[17–20]

The main objective of this investigation is twofold. First, we try to simplify the complexity in determining the internal pressure inside the spherical bubble by introducing a novel reduced order gas pressure law from the well-known fundamental equations in the uniform pressure approximation. This simplification is particularly essential for the simulation of bubbly cavitating flows using bubble dynamics models in complex geometries where reduced order models for the gas pressure inside the bubbles can enable realistic and computationally feasible solutions. The novel reduced gas pressure law obtained for single bubbles depends on the bubble wall temperature, the bubble radius, the Péclet number based on a characteristic time scale, and the isentropic exponent of the gas. This reduced order gas pressure law, which characterizes the change of state of the gas inside the bubble from nearly isothermal to nearly adiabatic conditions, also provides physical insight into how the characteristic time changes and thereby how the Péclet number changes during this transition in response to acoustic pressure signals. Second, we construct a simple acoustic cavitation model based on the novel reduced order gas pressure law for various applications by accounting for phase change but neglecting gas and vapor diffusion. To achieve these goals, we first consider the energy balance between a spherical gas bubble and the surrounding liquid, neglecting phase change and gas diffusion. In this case, we investigate the thermal behavior inside the bubble in the uniform pressure approximation by studying the well-known coupled equations for the gas pressure and temperature, which we attempt to solve iteratively. The first iteration, where the first order radial partial derivative of the temperature at the bubble wall is approximated by neglecting all higher order radial partial derivatives of the temperature at the bubble wall, shows that the gas pressure is a polytropic power law of the bubble wall temperature and the bubble radius, with the polytropic index given explicitly in terms of the isentropic exponent of the gas;[21] however, this first iterative reduced order gas pressure law turns out to be oversimplified since it lacks the dependence on the Péclet number. For this reason, iterative solutions that lead to hierarchy equations for the radial partial derivatives of the temperature at the bubble wall are constructed. These hierarchy equations are closed by a relation based on the ansatz that approximates the rapid change of state during collapse from almost isothermal to almost adiabatic behavior by time averaging the complex dynamics of change of state over a relatively short characteristic time. This, in turn, upon exact integration, yields the desired reduced order gas pressure law exhibiting power law dependence on the bubble wall temperature and on the bubble radius, with power indices depending on the isentropic exponent of the gas, the Péclet number, and a characteristic time scale through a parameter.[22] In particular, the reduced order gas pressure law yields the classical isothermal law when this parameter takes the value 1/2 and the bubble wall temperature assumes the value of the bulk liquid temperature for low Péclet numbers ($Pe \to 0$) and to the classical adiabatic pressure–radius relation when this parameter tends to infinity for high Péclet numbers ($Pe \to \infty$). The bubble wall temperature entering this reduced order gas pressure law can be obtained from the Plesset–Zwick solution[23] of the temperature distribution of the liquid side in the thin boundary layer approximation. The results for small amplitude oscillations of gas bubbles are recovered by identifying the parameter of the novel reduced order gas pressure law from the linear theory.[24–29] The novel gas pressure law is then validated against the near-isothermal solution of Prosperetti[12] by the numerical solution of the Keller–Miksis equation[30] for spherical bubble dynamics under near-isothermal conditions and constant bubble wall temperature. Numerical simulations of the original energy balance equations for gas bubbles are then carried out using spectral methods, and the results are compared to those obtained by the novel reduced order gas pressure law. Excellent agreement is reached for particular values of the model parameter. Using the novel reduced order gas pressure law, an acoustic cavitation model that couples spherical bubble dynamics by the Keller–Miksis equation to the Plesset–Zwick equation for the bubble wall temperature is constructed for noncondensable gas/vapor bubbles by accounting for phase change but neglecting mass diffusion. Results obtained for two different acoustically driven pressure signals show that the temporal variations of the bubble radius lie between those given by the classical isothermal and adiabatic laws as the parameter of the proposed acoustic model is varied. When constant interface properties (in particular, constant latent heat of vaporization) are employed, the bubble wall temperatures increase by an order of magnitude that suggest the use of variable interface properties in the proposed model. When variable interface properties are used, the bubble wall temperatures are reduced to reasonable values in agreement with the results of previous investigations.[14] Moreover, the comparison between the results obtained by the adiabatic law and those by the present acoustic cavitation model using sufficiently large values of the model parameter shows considerable differences in the bubble wall temperature variations in contrast to very good agreement in the bubble radius variations during initial growth and subsequent rebounds, implying that the perfect gas law is not satisfied at the interface due to phase change and the uniform pressure approximation.

## II. THERMAL DIFFUSION THROUGH A GAS BUBBLE IN THE UNIFORM PRESSURE APPROXIMATION

In this section, we focus on the thermal behavior inside the bubble in the uniform pressure approximation. The partial differential equation for the temperature field inside a gas bubble in the uniform pressure approximation is given by Prosperetti,[12] which can be written in normalized form[31] as

$$\frac{p}{T}\left\{\frac{\partial T}{\partial t}+\frac{1}{(Pe)\,p\,R^2}\left[\lambda(T)\frac{\partial T}{\partial y}-y\left(\frac{\partial T}{\partial y}\right)_{y=1^-}\right]\frac{\partial T}{\partial y}\right\} = \frac{(\gamma-1)}{\gamma}\frac{dp}{dt}+\frac{1}{(Pe)\,R^2\,y^2}\frac{\partial}{\partial y}\left[y^2\lambda(T)\frac{\partial T}{\partial y}\right]. \tag{1}$$

In Eq. (1), $T$ is the spherically symmetric temperature field inside the bubble, normalized with respect to the bulk liquid temperature $T_0'$; $p$ is the bubble gas pressure in the uniform pressure approximation, normalized with respect to a reference pressure $p_0'$; $R$ is the bubble radius, normalized with respect to the initial bubble radius $R_0'$; $\lambda(T)$ is the thermal conductivity of the gas, normalized with respect to its value $\lambda_R'$ at the bubble wall; $\gamma$ is the isentropic exponent of the gas; $y$

is the radial coordinate, measured from the bubble center and normalized with respect to the instantaneous value of the bubble radius; and $t$ is the time, normalized with respect to a typical characteristic time scale $\Theta'$. The Péclet number $Pe$ is based on the characteristic time scale $\Theta'$ and is defined by

$$Pe = \frac{\gamma p_0' R_0'^2}{(\gamma-1)\lambda_R' T_0' \Theta'}, \tag{2}$$

which is physically described as the ratio of the diffusion time scale to the advection time scale. The gas pressure in the uniform pressure approximation can then be found by solving the differential equation

$$\frac{dp}{dt} = \frac{3\gamma}{R}\left[\frac{1}{(Pe)\,R}\left(\frac{\partial T}{\partial y}\right)_{y=1^-} - p\frac{dR}{dt}\right], \tag{3}$$

which requires the solution of Eq. (1) together with the initial and boundary conditions

$$T(t=0,y)=1, \quad T(t,y=1^-)=T_R(t), \quad \text{and} \quad \left(\frac{\partial T}{\partial y}\right)_{y=0}=0 \tag{4}$$

for the evaluation of the bubble wall radial temperature gradient $c(t;Pe)=(\partial T/\partial y)_{y=1^-}$. It is important to mention that in arriving at Eq. (3), no gas transport is allowed across the gas–liquid interface. With this in mind, Eqs. (1) and (3) should be solved simultaneously satisfying the initial and boundary conditions of the gas temperature given by Eq. (4) together with an initial condition for the gas pressure, supplemented by the solution of a spherical bubble dynamics equation for the bubble radius.

In the rest of this paper, we derive a hierarchy of equations for the radial partial derivatives of the gas temperature at the bubble wall by carrying out a series expansion of the gas temperature near the bubble wall and by substituting it into the energy equation (1). We then introduce a closure relation for the hierarchy equations by time averaging the complex dynamics of change of state over a characteristic time, arriving at the reduced order gas pressure law by exact integration of Eq. (3). This novel reduced order gas pressure law depends on the bubble radius $R(t)$ (to be obtained by solving the Keller–Miksis equation of spherical bubble dynamics), the bubble wall temperature $T_R(t)$ (to be obtained from the Plesset–Zwick solution in Sec. III), and a parameter that is a function of the Péclet number and characteristic time. Consequently, an acoustic cavitation model based on the novel reduced order gas pressure law is constructed in Sec. IV, and the results of the model for air bubbles in water are presented in Sec. VI.

### A. From isothermal to adiabatic change of state: Hierarchy equations for the radial partial derivatives of the gas temperature at the bubble wall

It is well-known from earlier numerical simulations[9,10] that the initial growth of the bubble is almost isothermal and that its final collapse stage before rebound can exhibit almost adiabatic behavior. To achieve such a change of state, we here adapt an iterative method of solution by first carrying out an expansion for the temperature field of the gas inside the bubble near the bubble wall as

$$T(t,y) = T_R(t) + \left(\frac{\partial T}{\partial y}\right)_{y=1^-}(y-1^-) + \frac{1}{2!}\left(\frac{\partial^2 T}{\partial y^2}\right)_{y=1^-}(y-1^-)^2 + \cdots \tag{5}$$

together with a similar expansion for the thermal conductivity of the gas

$$\lambda(T) = \lambda(T_R) + \left(\frac{d\lambda}{dT}\right)_R\left(\frac{\partial T}{\partial y}\right)_{y=1^-}(y-1^-) + \frac{1}{2!}\left[\left(\frac{d^2\lambda}{dT^2}\right)_R\left(\frac{\partial T}{\partial y}\right)^2_{y=1^-} + \left(\frac{d\lambda}{dT}\right)_R\left(\frac{\partial^2 T}{\partial y^2}\right)_{y=1^-}\right] \times (y-1^-)^2 + \cdots, \tag{6}$$

where $(d\lambda/dT)_R = (d\lambda/dT)_{y=1^-}$. Truncating the series expansions (5) and (6) after two or three terms within a reasonable error would yield results valid only for the near-isothermal change of state, implying a relatively large near isothermal characteristic time scale $\Theta'_{nis}$ with $Pe \ll 1$. If a transition from a near isothermal ($Pe \ll 1$) to a near adiabatic ($Pe \gg 1$) change of state is to be considered, the series expansions given by Eqs. (5) and (6) have to be truncated after some finite N-terms for convergence, N depending on the Péclet number $Pe$. Therefore, the adiabatic change of state [$Pe \to \infty$, where all terms in the series become of the same order of magnitude, and thus, the series given by Eq. (5) diverges] is not considered. Substitution of the above expansions into Eq. (1) and taking the limit $y \to 1^-$ lead to the following quadratic equation for the bubble wall gas temperature gradient $c(t;Pe)$:

$$\left(\frac{d\lambda}{dT}\right)_R c^2(t;Pe) + 2\,c(t;Pe) - \left\{(Pe)\,p\,R^2 \times \left[\frac{1}{T_R}\frac{dT_R}{dt} - \frac{(\gamma-1)}{\gamma}\frac{1}{p}\frac{dp}{dt}\right] - \left(\frac{\partial^2 T}{\partial y^2}\right)_{y=1^-}\right\} = 0. \tag{7}$$

The solution of the quadratic equation for $c$ yields the first hierarchy equation between the first order and second order radial partial derivatives of the temperature at the bubble wall as

$$c(t;Pe) = \frac{-1+\sqrt{1+\left(\frac{d\lambda}{dT}\right)_R\left\{(Pe)\,p\,R^2\left[\frac{1}{T_R}\frac{dT_R}{dt} - \frac{(\gamma-1)}{\gamma}\frac{1}{p}\frac{dp}{dt}\right] - \left(\frac{\partial^2 T}{\partial y^2}\right)_{y=1^-}\right\}}}{\left(\frac{d\lambda}{dT}\right)_R}. \tag{8}$$

When the temperature dependence of the thermal conductivity is neglected, the first hierarchy equation (8) simplifies to

$$c(t;Pe) = \left(\frac{\partial T}{\partial y}\right)_{y=1^-} = \frac{(Pe)\,R^2}{2}\left[\frac{p}{T_R}\frac{dT_R}{dt} - \frac{(\gamma-1)}{\gamma}\frac{dp}{dt}\right] - \frac{1}{2}\left(\frac{\partial^2 T}{\partial y^2}\right)_{y=1^-}. \tag{9}$$

Equation (9) shows that the radial temperature gradient at the bubble wall depends on the bubble radius, the bubble wall temperature, and the gas pressure as well as on the second order radial partial derivative of the gas temperature at the bubble wall. Therefore, we require the value of the second order radial partial derivative of the gas temperature at the bubble wall in order to be able to solve for the gas pressure from Eq. (3) using Eq. (9). For this reason, we differentiate Eq. (1) with respect to $y$ and take the limit $y \to 1^-$ to arrive at the second hierarchy equation between the second order and third order radial partial derivatives of the temperature at the bubble wall,

$$\left(\frac{\partial^2 T}{\partial y^2}\right)_{y=1^-} = c\left[1 + \frac{(Pe)\,p\,R^2}{2\,T_R}\frac{d}{dt}\ln\left|\frac{c/(2\,T_R)}{1-c/(2\,T_R)}\right|\right] - \frac{1}{2\left(1-\frac{c}{2\,T_R}\right)}\left(\frac{\partial^3 T}{\partial y^3}\right)_{y=1^-}, \tag{10}$$

where the temperature dependence of the non-dimensional thermal conductivity $\lambda(T)$ in Eq. (1) is left out. Similarly, we find the third hierarchy equation between the third order and fourth order radial partial derivatives of the temperature at the bubble wall as

$$\begin{aligned}\left(\frac{\partial^3 T}{\partial y^3}\right)_{y=1^-} = \frac{c}{(2\,T_R - c)}\Bigg\{ & \frac{(Pe)^2\,p^2\,R^4}{c\,T_R}\left(\frac{d^2T_R}{dt^2}\right) + \frac{3\,(\gamma-1)\,(Pe)^2\,p^2\,R^3}{c}\left(\frac{d^2R}{dt^2}\right) \\ & + \frac{(6\gamma-7)\,(Pe)^2\,p^2\,R^3}{c\,T_R}\left(\frac{dT_R}{dt}\right)\left(\frac{dR}{dt}\right) + \frac{3\,(\gamma-1)\,(3\gamma-5)\,(Pe)^2\,p^2\,R^2}{c}\left(\frac{dR}{dt}\right)^2 \\ & + 3\,(\gamma-1)\,(Pe)\,pR\left[\frac{4T_R}{c} - \frac{2c}{T_R} - 9\gamma + 2\right]\left(\frac{dR}{dt}\right) + (Pe)\,pR^2\left[\frac{4}{c} - \frac{(6\gamma-1)}{T_R}\right]\left(\frac{dT_R}{dt}\right) \\ & - (Pe)\,pR^2\left[\frac{2}{T_R} + \frac{(3\gamma-1)}{c}\right]\left(\frac{dc}{dt}\right) - 12\,\gamma\,T_R + 6\,\gamma\,(3\,\gamma-1)\,c + \frac{6\gamma}{T_R}\,c^2\Bigg\} - \frac{1}{2\left(1-\frac{c}{2\,T_R}\right)}\left(\frac{\partial^4 T}{\partial y^4}\right)_{y=1^-}. \end{aligned} \tag{11}$$

It is now clear that we need the fourth order partial derivative of the temperature at the bubble wall in order to be able to solve for the gas pressure. In principle, one can obtain higher (fourth order, fifth order, etc.) hierarchy equations by differentiating Eq. (1) with respect to the non-dimensional radial coordinate $y$ successively (three times, four times, etc.) and by taking the limit $y \to 1^-$ afterward, leaving out the temperature dependence of the thermal conductivity. In this manner, one can construct an infinite sequence of hierarchy equations relating the $n$th order and the $(n+1)$-th order radial partial derivatives of the gas temperature at the bubble wall in the form

$$\left(\frac{\partial^n T}{\partial y^n}\right)_{y=1^-} = c(t;Pe)\,F_n(t;Pe) + G_n(t;Pe)\left(\frac{\partial^{n+1} T}{\partial y^{n+1}}\right)_{y=1^-}, \quad n = 2,3,4,\ldots. \tag{12}$$

In particular, for $n = 2$ and $n = 3$, the functions $F_2(t;Pe)$, $G_2(t;Pe)$ and $F_3(t;Pe)$, $G_3(t;Pe)$ can easily be identified from the second and third hierarchy equations (10) and (11), respectively. In principle, beginning with the second hierarchy equation (10), one can successively substitute for the higher order radial partial derivatives of the temperature at the bubble wall to arrive at

$$\begin{aligned}\left(\frac{\partial^2 T}{\partial y^2}\right)_{y=1^-} &= c(t;Pe)\left[F_2(t;Pe) + \sum_{j=2}^{n-1} F_{j+1}(t;Pe) \times \left(\prod_{i=2}^{j} G_i(t;Pe)\right)\right] + \left(\prod_{i=2}^{n} G_i(t;Pe)\right)\left(\frac{\partial^{n+1} T}{\partial y^{n+1}}\right)_{y=1^-} \end{aligned} \tag{13}$$

for $n \geq 3$. On the other hand, in the limit as $n \to \infty$, we would have pointwise convergence of the infinite sequence of the radial partial derivatives of the gas temperature at the bubble wall so that, in this limit, Eq. (12) yields

$$\lim_{n\to\infty}\left(\frac{\partial^n T}{\partial y^n}\right)_{y=1^-} = c(t;Pe)\lim_{n\to\infty}\frac{F_n(t;Pe)}{1-G_n(t;Pe)}. \tag{14}$$

Now, by taking the limit as $n \to \infty$ of Eq. (13) and by utilizing Eq. (14), one can, in principle, obtain the expression

$$\begin{aligned}\left(\frac{\partial^2 T}{\partial y^2}\right)_{y=1^-} &= 2\,c(t;Pe)\,H(t;Pe) \\ &= c(t;Pe)\left\{F_2(t;Pe) + \lim_{n\to\infty}\left[\sum_{j=2}^{n-1} F_{j+1}(t;Pe) \times \left(\prod_{i=2}^{j} G_i(t;Pe)\right) + \frac{F_n(t;Pe)}{1-G_n(t;Pe)}\left(\prod_{i=2}^{n} G_i(t;Pe)\right)\right]\right\}, \end{aligned} \tag{15}$$

which defines the function $H(t;Pe)$. Now, substitution from Eq. (15) for $\left(\frac{\partial^2 T}{\partial y^2}\right)_{y=1^-}$ into the first hierarchy equation (9) yields the exact expression for $c(t;Pe)$ as

$$c(t;Pe) = \left(\frac{\partial T}{\partial y}\right)_{y=1^-} = \frac{(Pe)R^2}{2[1+H(t;Pe)]}\left[\frac{p}{T_R}\frac{dT_R}{dt} - \frac{(\gamma-1)}{\gamma}\frac{dp}{dt}\right]. \tag{16}$$

Consequently, the exact solution for the gas pressure in the uniform pressure approximation can be obtained by substituting from Eq. (16) for $c(t;Pe)$ into Eq. (3) and solving the resulting ordinary differential equation (ODE) coupled to the evolution equations of the bubble wall temperature $T_R(t)$ and the bubble radius $R(t)$, provided that the function $H(t;Pe)$ is known. However, it is almost impossible to obtain the limiting function $H(t;Pe)$ defined by Eq. (15) explicitly since this would require knowledge of the infinite sequence of all functions entering the hierarchy equations for the radial partial derivatives of the temperature at the bubble wall. Nevertheless, some information can be obtained from the Péclet number dependence for the change of state from isothermal to adiabatic behavior. The function $H(t;Pe)$, which characterizes possible changes due to nonlinear advection and thermal diffusion inside the bubble, remains finite when the Péclet number is relatively small in magnitude (the near isothermal approximation) since the Taylor series given by Eq. (5) can then be truncated after a few terms. However, the function $H(t;Pe)$ becomes unbounded in the adiabatic limit as $Pe \to \infty$. In this limit, all terms in the series become of the same order of magnitude so that the series given by Eq. (5) diverges (this means that the adiabatic limit can be reached only asymptotically). In Subsection II B, these characteristics of the function $H(t;Pe)$ will be exploited for the closure of the hierarchy equations.

With this in mind, we now discuss the limiting isothermal and adiabatic change of states. Independent of the value of the Péclet number $Pe$ [and therefore, of the function $H(t;Pe)$], we first distinguish the special case where $T_R(t)$ = constant = $T_c$ and $\gamma = 1$, with $T_c$ denoting the normalized critical temperature of the gas, which presumably can be realized at the thermodynamic critical point. In this case, the change of state is both isothermal and adiabatic.

#### 1. The isothermal change of state

In this case, $T_R(t)$ = constant by definition. Besides the special case discussed above, it follows that this can only be realized in the limit as $Pe \to 0$ (or the isothermal characteristic time $\Theta' = \Theta'_{is} \to \infty$). In this limit, substitution from Eq. (16) into Eq. (3) shows that the isothermal change of state is realized if and only if the function $H(t;0)$ assumes the constant value 1/2.

#### 2. The adiabatic change of state

In this case, $c = 0$ by definition. Independent of the value of the Péclet number $Pe$, it follows from Eq. (16) that this change of state is naturally satisfied by the isentropic pressure–temperature relation of the gas ($p \propto T_R^{\gamma/(\gamma-1)}$), and it consistently yields the adiabatic pressure–radius relation $pR^{3\gamma}$ = constant upon integration of Eq. (3) together with $c = 0$. However, as mentioned above in the preceding paragraph, in the adiabatic limit ($c = 0$), the pressure–radius relation $pR^{3\gamma}$ = constant can also be realized as the function $H(t;Pe)$ becomes unbounded, which is physically realized in the limit as $Pe \to \infty$ (or the adiabatic characteristic time $\Theta' = \Theta'_{ad} \to 0$). In this case, we also obtain the adiabatic pressure–radius relation $pR^{3\gamma}$ = constant upon exact integration of Eq. (3) but not necessarily satisfying the isentropic pressure–temperature relation (violation of the ideal gas equation at the gas/liquid interface). This case has also been discussed in the theory of single bubble sonoluminescence.[32]

Equations (1), (3), and (16) together with an approximation for the function $H(t;Pe)$ can now be solved iteratively for the gas temperature and gas pressure utilizing the initial and boundary conditions for the gas temperature and an initial condition for the gas pressure, provided that the bubble wall temperature $T_R(t)$ and the bubble radius $R(t)$ are known. In what follows, the function $H(t;Pe)$ will be approximated by its average value over a characteristic time, the bubble wall temperature $T_R(t)$ will be obtained from the solution of the thermal diffusion equation of the liquid side by utilizing the interface conditions, and the bubble radius $R(t)$ will be evaluated from the solution of a Rayleigh–Plesset type bubble dynamics equation with appropriate initial conditions.

### B. Closure of the hierarchy equations: A reduced order gas pressure law

It is well-known from early numerical simulations[9,10] that the initial growth of a bubble in thermodynamic equilibrium excited by an acoustic pressure signal is almost isothermal and that its final collapse stage before rebound may exhibit adiabatic behavior. The growth and collapse of the bubble followed by subsequent rebounds usually involve multiple characteristic time scales, resulting in different Péclet numbers for growth and collapse. Actually, the change in characteristic time scale reflects on the change in magnitude of the value of the function $H(t;Pe)$ from 1/2 ($Pe \to 0$ implying isothermal change of state) to infinity ($Pe \to \infty$ implying adiabatic change of state). It is thus expected that the function $H(t;Pe)$ can vary considerably with time. In order to get around this difficulty, we select a typical normalized characteristic time scale $\vartheta$, which is likely to reflect the mean behavior of the change of state of the gas. It may now be possible to capture the dominant features of the nonlinear advection and thermal diffusion effects on bubble motion by averaging the function $H(t;Pe)$ during this characteristic time. If we denote by $t_1$ the normalized time where the function $H(t;Pe)$ begins to deviate from its isothermal behavior and by $t_2 = t_1 + \vartheta$ the normalized time just after the characteristic time period, we can define the average value $f(Pe;\vartheta)$ of the function $H(t;Pe)$ over the characteristic interval $(t_1, t_2)$ as

$$f(Pe;\vartheta) = \frac{1}{\vartheta}\int_{t_1}^{t_1+\vartheta} H(t;Pe)\,dt, \tag{17}$$

where the normalized characteristic time is $\vartheta = (t'_2 - t'_1)/\Theta' = t_2 - t_1$. We can now approximate $H(t,Pe)$ by its average value $f(Pe;\vartheta)$ so that the radial temperature gradient at the bubble wall $c(t;Pe)$ given by Eq. (16) becomes

$$c(t;Pe) = \left(\frac{\partial T}{\partial y}\right)_{y=1^-} = \frac{(Pe)\,R^2}{2\,[1+f(Pe;\vartheta)]}\left[\frac{p}{T_R}\frac{dT_R}{dt} - \frac{(\gamma-1)}{\gamma}\frac{dp}{dt}\right]. \tag{18}$$

Furthermore, if we substitute from Eq. (18) for $c(t;Pe)$ into Eq. (3), upon exact integration, we arrive at the reduced order gas pressure

law in the form

$$p = p_{g0}\left[\frac{(T_R)^{1/2(1+f)}}{R}\right]^{3\Gamma}, \tag{19}$$

where the polytropic exponent $\Gamma$ in this case is given by

$$\Gamma = \frac{2\gamma(1+f)}{(3\gamma-1+2f)}, \tag{20}$$

where $1/2 < f = f(Pe;\vartheta) < \infty$. Figure 1 shows the variation of the polytropic exponent $\Gamma$ against the function $f$ for air ($\gamma = 1.4$) and for a monatomic gas ($\gamma = 5/3$). Independent of the bubble wall temperature $T_R$, it can be shown that the reduced order gas pressure law given by Eqs. (19) and (20) reduces to the classical adiabatic pressure–radius relation as $f \to \infty$, which is known to be valid as $Pe \to \infty$. One can also show that for $f = 1/2$ and $T_R = 1$, the classical isothermal law, valid as $Pe \to 0$, is recovered. From physical considerations, it is now obvious that the function $f(Pe;\vartheta)$ is an increasing function of Péclet number $Pe$. Depending on the value of the characteristic time $\vartheta$ (or Péclet number $Pe$), we can now distinguish three different regimes of change of state.

### 1. The nearly isothermal change of state

This is realized when the characteristic time is large enough implying small Péclet number ($Pe \ll 1$). Thus, in this case, the function $f(Pe;\vartheta)$ is near the isothermal value 1/2 [say $1/2 < f = f(Pe;\vartheta) < 1$].

### 2. The nearly adiabatic change of state

This is realized when the characteristic time is small enough, implying large Péclet number ($Pe \gg 1$). Thus, in this case, the function $f(Pe;\vartheta) \gg 1$ (say $f > 10$ for air and $f > 15$ for a monatomic gas, referring to Fig. 1).

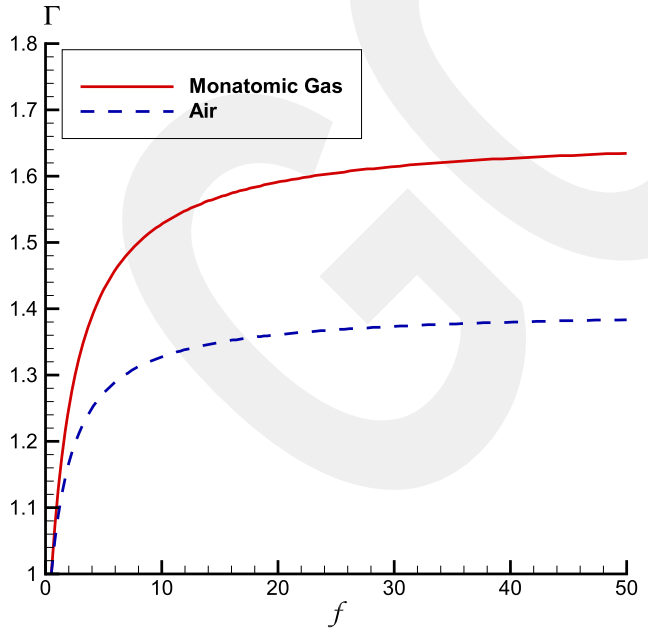


**FIG. 1.** Variation of the function $\Gamma$ given by Eq. (20) with respect to $f$ for air and for a monatomic gas.

### 3. The transition change of state

This is realized when the characteristic time is of the order of unity in magnitude [$\vartheta = O(1)$], implying a Péclet number being of the order of unity [$Pe = O(1)$]. Thus, in this case, the function $f(Pe;\vartheta) = O(1)$ [say $1 < f = f(Pe;\vartheta) < 10$ for air and $1 < f = f(Pe;\vartheta) < 15$ for a monatomic gas, referring to Fig. 1].

In general, the change of state during the growth and collapse of the bubble may involve a sequence of the above regimes with multiple characteristic times (corresponding to different Péclet numbers) for averaging the function $H(t;Pe)$ over different characteristic times. In what follows, for simplicity, we choose a single characteristic time (corresponding to a fixed Péclet number) for averaging the function $H(t;Pe)$, resulting in an optimized change of state. Moreover, in cases where the difference between the bubble wall temperature and the bulk liquid temperature is sufficiently small, the bubble wall temperature can be taken as the bulk liquid temperature.[9,12] The reduced order gas pressure law then takes the simplified form

$$p = \frac{p_{g0}}{R^{3\Gamma}}, \tag{21}$$

where the polytropic exponent $\Gamma$ is given by Eq. (20). In this case, the isothermal law is recovered when $f = 1/2$ and the adiabatic pressure–radius relation is approached as $f \to \infty$. The simplified reduced order gas pressure given by Eq. (21) can be very useful for bubble dynamic models where the bubble wall temperature is near the bulk liquid temperature and where simplifications are necessary to avoid long computation times. Estimates of the function $f$ depending on the Péclet number $Pe$ and on the normalized characteristic time $\vartheta$ are discussed in Sec. V.

## III. THERMAL DIFFUSION IN THE SURROUNDING LIQUID: THE PLESSET–ZWICK SOLUTION

The bubble wall temperature can be significantly different from the ambient liquid temperature, especially during the violent collapse of the bubble. In such a case, the consideration of the energy equation in the surrounding liquid is essential. If $T_\ell(y,t)$ denotes the temperature distribution inside the liquid phase, normalized with respect to the ambient liquid temperature $T_0'$, at time $t$ and at a normalized distance $y = r'/R' \geq 1$, where $r'$ is the radial distance from the bubble center, the energy equation in the liquid can be written as[1]

$$\frac{\partial T_\ell}{\partial t} + \frac{R^2}{y^2}\frac{dR}{dt}\frac{\partial T_\ell}{\partial y} = \left(\frac{\alpha_{\ell 0}'\,\Theta'}{R_0'^{\,2}}\right)\frac{1}{R^2\,y^2}\frac{\partial}{\partial y}\left(y^2\frac{\partial T_\ell}{\partial y}\right), \tag{22}$$

where $\alpha_{\ell 0}'$ is the thermal diffusivity of the liquid at the cold liquid temperature, $R_0'$ is the initial bubble radius, and $\Theta'$ is a characteristic time. Assuming that the bubble wall temperature is continuous across the gas/liquid interface [$T_R = (T_\ell)_{y=1^+}$], the normalized bubble wall temperature $T_R$ can be obtained by the Plesset and Zwick[23] solution

$$T_R(t) = 1 - \left(\frac{\alpha_{\ell 0}'\,\Theta'}{\pi R_0'^{\,2}}\right)^{1/2}\int_0^t \frac{R(\xi)(\partial T_\ell/\partial y)_{y=1^+}}{\left[\int_\xi^t R^4(\tau)d\tau\right]^{1/2}}d\xi. \tag{23}$$

Equation (23) relates the bubble wall temperature $T_R$ to bubble dynamics and to the heat flux at the bubble wall conducted to the

liquid through the bubble wall. For a gas bubble, the heat flux at the bubble wall is also continuous, relating the radial liquid temperature to the radial gas temperature gradient $c(t;Pe)$ at the bubble by

$$\left(\frac{\partial T_\ell}{\partial y}\right)_{y=1^+} = \left(\frac{\lambda'(T_R')}{\lambda_\ell'(T_R')}\right)\left(\frac{\partial T}{\partial y}\right)_{y=1^-} = A\, c(t;Pe), \tag{24}$$

where $A = (\lambda'(T_R')/\lambda_\ell'(T_R'))$ denotes the ratio of the gas thermal conductivity to that of the liquid at the bubble wall. Substitution from Eq. (24) for $(\partial T_\ell/\partial y)_{y=1^+}$ into Eq. (23) yields

$$T_R(t) = 1 - \left(\frac{\alpha_{\ell 0}'\,\Theta'}{\pi R_0'^2}\right)^{1/2} \int_0^t \frac{R(\xi)\,A(\xi)\,c(\xi;Pe)}{\left[\int_\xi^t R^4(\tau)d\tau\right]^{1/2}} d\xi. \tag{25}$$

Equations (18)–(20) and (25) coupled to spherical bubble dynamics form an integro-differential system for the uniform gas pressure $p(t)$ within the bubble and for the bubble wall temperature $T_R(t)$ and can be solved iteratively by employing a Rayleigh–Plesset type equation for spherical bubble dynamics.

## IV. A REDUCED ORDER ACOUSTIC CAVITATION MODEL

In this section, we consider acoustic cavitation (gas–vapor) bubbles where the mixture pressure $p_b$ inside the bubble is taken as the sum of the partial vapor pressure $p_v$ and the partial gas pressure $p_g$ assuming a gas mixture of ideal gases, which in normalized form can be written as

$$p_b = p_v + p_g. \tag{26}$$

Within the framework of the uniform pressure approximation, the normalized vapor pressure can be taken as the normalized saturation vapor pressure at the normalized bubble wall temperature $T_R$, i.e., $p_v = p_{v,sat}(T_R)$. In order to be able to use the results of the reduced order model of Sec. II for the normalized gas pressure $p_g$, it is important to note that no mass transport between the bubble and the surrounding liquid is allowed at the bubble wall in the balance equations (1) and (3). For gas–vapor bubbles, in general, mass transport for the noncondensable gas and phase change (evaporation/condensation) at the bubble wall should be taken into account. Thus, Eqs. (1) and (3), and consequently, the reduced order gas pressure law given by Eqs. (19) and (20), have to be modified when phase change and mass transport effects between the bubble and the surrounding liquid become comparable to that of thermal conduction through the bubble wall. Recently, a reduced order, single bubble acoustic cavitation model that takes into account heat as well as mass transfer with uniform spatial distribution of thermodynamic variables everywhere except within boundary layers near the bubble wall has been carried out by Kreider *et al.*[16] utilizing an ODE similar to Eq. (3) for the time rate of change of the mixture pressure modified by the effect of mass transfer of the gas and vapor. However, as the authors state, experimental observations were used to tune and test model parameters. We herein construct a simple reduced-order acoustic cavitation model, based on the results of Secs. II and III, which aim to fulfill the need for avoiding lengthy and expensive numerical simulations of the complex multiphase flow equations together with interface conditions for cases where the assumptions and simplifications made remain valid. For this reason, we first assume an insoluble noncondensable gas where the solubility of the gas in the liquid is small enough not to effect bubble dynamics and the thermodynamic state of the multiphase mixture (such an assumption is valid for air bubbles in water at room temperature[14]). This simplification already enables us to avoid solving the diffusion equation for the air concentration in the liquid, similar to Eq. (22) where the liquid temperature is replaced by the non-condensable concentration and the thermal diffusivity of the liquid is replaced by the diffusion coefficient of the noncondensable gas in the liquid together with the interfacial Henry law condition. Despite this simplification for the air–water system, the effect of the vapor mass transfer at the interface due to evaporation and condensation has to be taken into account in the balance equations (1) and (3) for gas–vapor bubbles. For this reason, we first discuss the interfacial conditions for the temperature. We still assume the continuity of the temperature at the interface, i.e., the equality of the temperatures of the gas–vapor mixture and of the liquid at the interface ($T_R = T_{\ell R}$), as usually accepted (Kreider *et al.*[16] also discussed the case of a temperature jump with a temperature-jump coefficient at the gas–liquid interface in their reduced order model, but they are skeptical in extrapolating the temperature jump coefficient from kinetic theory). However, the continuity of the heat flux at the gas–liquid interface given by Eq. (24) for gas bubbles is no longer valid due to evaporation and condensation at the gas–liquid interface and has to be replaced by the normalized condition

$$\left(\frac{\partial T_\ell}{\partial y}\right)_{y=1^+} - \left(\frac{\lambda_b'(T_R')}{\lambda_\ell'(T_R')}\right)\left(\frac{\partial T}{\partial y}\right)_{y=1^-} = \left(\frac{R_0' m_v'' L'(T_R')}{T_0' \lambda_\ell'(T_R')}\right) R, \tag{27}$$

where $L'(T_R')$ is the latent heat of condensation at the bubble wall temperature, $\lambda_b'(T_R')$ is the thermal conductivity of the gas–vapor mixture at the interface, $\lambda_\ell'(T_R')$ is the thermal conductivity of the liquid at the interface, and $m_v''$ is the vapor mass flux across the interface (it is positive for flow into the bubble during evaporation). The vapor mass flux at the interface is, in principle, determined from kinetic theory;[9,14,16] however, the value of the accommodation equation to be used, which is usually obtained from molecular simulations under different conditions, presents a serious difficulty. Here, we, instead, determine the vapor mass flux $m_v''$ using an approximate lumped energy balance at the interface. In this balance, we can assume that the heat supplied from the liquid to the interface during growth is almost totally used for vaporization and that the heat released by condensation during collapse is almost totally transferred from the interface to the liquid by neglecting the heat used in heating or cooling the bubble contents since the thermal conductivity of the liquid is much larger in magnitude than that of the vapor. Therefore, one can relate the rate of change of vapor mass production to the rate of change of volume increase arriving at the normalized relation[1,31,33]

$$\frac{\rho'_{v0,sat}L'(T'_R)}{3\Theta'}\frac{d}{dt}\left[\rho_{v,sat}(T_R)R^3\right]=\left(\frac{T'_0\lambda'_\ell(T'_R)}{R'^2_0}\right)R\left(\frac{\partial T_\ell}{\partial y}\right)_{y=1^+}, \quad (28)$$

where $\rho_{v,sat}(T_R)=\rho'_{v,sat}(T'_R)/\rho'_{v0,sat}$ is the normalized saturated vapor density evaluated at the bubble wall temperature, with $\rho'_{v0,sat}$ denoting the saturated vapor density at the bulk liquid temperature. Within this approximation, the vapor mass flux $m''_v$ can be written as

$$m''_v=\left(\frac{R'_0\,\rho'_{v0,sat}}{3\,\Theta'}\right)\frac{1}{R^2}\frac{d}{dt}\left[\rho_{v,sat}(T_R)\,R^3\right] \quad (29)$$

by eliminating $(\partial T_\ell/\partial y)_{y=1^+}$ between Eqs. (27) and (28). If we further assume that the rate of vapor mass transfer to or from the bubble is small enough to change the initial vapor concentration $\mathcal{C}_0$ within the bubble, the energy balance equations (1) and (3) can be modified to include the effect of the initial vapor concentration $\mathcal{C}_0$ for gas–vapor bubbles. From the modified balance equations [Eqs. (A1) and (A2) in Appendix A], we can now identify the validity of the reduced order gas pressure law given by Eq. (19) in Sec. II as the condition given by Eq. (A8), as worked out in detail in Appendix A. Under these conditions, the normalized bubble mixture pressure $p_b$ can now be written as

$$p_b=p_v+p_g=p_{v,sat}(T_R)+p_{g0}\left[\frac{(T_R)^{1/2(1+f)}}{R^{1-\mathcal{C}_0}}\right]^{3\,\Gamma}, \quad (30)$$

where $p_{v,sat}(T_R)$ is the normalized saturated vapor pressure at the bubble wall, $p_{g0}$ is the initial normalized partial gas pressure, and $\Gamma$ is given by Eq. (20). For the normalized bubble wall temperature $T_R$, we can still employ the Plesset–Zwick equation (23). Substituting for the normalized bubble wall temperature gradient of the liquid side from Eq. (28) together with Eq. (29) into the Plesset–Zwick equation (23), we obtain

$$T_R(t)=1-\mathcal{B}\int_0^t\frac{L(\xi)\left[\rho_{v,sat}(\xi)\,R^2(\xi)\,(dR/d\xi)+R^3(\xi)\,(d\rho_{v,sat}/dT_R)\,(dT_R/d\xi)/3\right]}{\lambda_\ell(\xi)\,\left[\int_\xi^t R^4(\tau)d\tau\right]^{1/2}}d\xi \quad (31)$$

for acoustic cavitation bubbles. In the above equation, the dimensionless constant $\mathcal{B}$ is given by

$$\mathcal{B}=\left(\frac{L'_0}{T'_0\,c'_{p\ell 0}}\right)\left(\frac{\rho'_{v0,sat}}{\rho'_{\ell 0}}\right)\frac{R'_0}{(\pi\,\Theta'\,\alpha'_{\ell 0})^{1/2}}, \quad (32)$$

where $c'_{p\ell 0}$ and $\rho'_{\ell 0}$ are, respectively, the specific heat of the liquid and the density of the liquid at the cold liquid temperature, with $L'_0$ and $\rho'_{v0,sat}$ denoting, respectively, the latent heat of condensation and the saturated vapor density at the cold liquid temperature, and $L(T_R)=L'(T'_R)/L'_0$ is the normalized latent heat of condensation at the bubble wall, $\rho_{v,sat}(T_R)=\rho'_{v,sat}(T'_R)/\rho'_{v0,sat}$ is the normalized saturated vapor density at the bubble wall, and $\lambda_\ell(T_R)=\lambda'_\ell(T'_R)/\lambda'_{\ell 0}$ is the normalized thermal conductivity of the liquid at the bubble wall temperature, with $\lambda'_{\ell 0}$ denoting its value at the cold liquid temperature. For liquids of negligible heating/cooling rates, the second term in the numerator of the integrand in Eq. (31) can be neglected. Equations (30)–(32) form the model equations of the reduced order gas pressure law for acoustic cavitation bubbles coupled to spherical bubble dynamics that accounts for liquid compressibility. Several equations of spherical bubble dynamics that account for liquid compressibility[30,34,35] have been proposed. Prosperetti and Lezzi[36] shown that all belong to a family of spherical bubble dynamic models obtained by the asymptotic expansion of the small wall Mach number corresponding to weak compressibility of a barotropic liquid ignoring thermal effects in the liquid. Nevertheless, as pointed out by Prosperetti and Lezzi[36] and exploited by Ando *et al.*,[37] the use of Gilmore's equation for spherical bubble dynamics in a compressible liquid yields more accurate results because the speed of sound is not taken to be constant but depends on the liquid pressure. In this study, we use the Keller–Miksis equation[30] for a weak compressible liquid, which takes the normalized form

$$\begin{aligned}&\left[1-M\dot{R}+\frac{4M}{R\,\mathrm{Re}(T_R)}\right]R\ddot{R}+\frac{3}{2}\left[1-\frac{M}{3}\dot{R}-\frac{8M}{3\,\mathrm{Re}(T_R)\,R}\right]\dot{R}^2+\left[\frac{4(1+M\dot{R})}{Re(T_R)}-\frac{2M}{We(T_R)}\right]\frac{\dot{R}}{R}\\&+2\,(1+M\dot{R})\left\{\frac{1}{R\,We(T_R)}-\frac{1}{We(1)}\left[\frac{(T_R)^{1/2(1+f)}}{R^{1-\mathcal{C}_0}}\right]^{3\,\Gamma}\right\}+\frac{(1+M\dot{R})}{2}\left\{\sigma(T_R)-\sigma(1)\left[\frac{(T_R)^{1/2(1+f)}}{R^{1-\mathcal{C}_0}}\right]^{3\,\Gamma}\right\}+\frac{(1+M\dot{R})\mathcal{C}_p}{2}\\&+\frac{MR}{2}\frac{dC_p}{dt}-\left(\frac{2}{We(1)}+\frac{\sigma(1)}{2}\right)M\,R\,\frac{d}{dt}\left[\frac{(T_R)^{1/2(1+f)}}{R^{1-\mathcal{C}_0}}\right]^{3\,\Gamma}+\frac{MR}{2}\frac{d\sigma}{dT_R}\frac{dT_R}{dt}-\frac{2M}{[We(T_R)]^2}\frac{dWe}{dT_R}\frac{dT_R}{dt}-\frac{4M\,\dot{R}}{[\mathrm{Re}(T_R)]^2}\frac{dRe}{dT_R}\frac{dT_R}{dt}=0,\end{aligned} \quad (33)$$

where $M = U_0'/a_{\ell 0}'$ is a characteristic Mach number, with $a_{\ell 0}'$ denoting the speed of sound in the liquid at the cold liquid temperature, $\sigma(T_R)$ is the cavitation number, $Re(T_R)$ is a typical Reynolds number, and $We(T_R)$ is the Weber number, all evaluated at the normalized bubble wall temperature, which are defined by

$$\sigma(T_R) = \frac{p_0' - p_{v,sat}'(T_R')}{\frac{1}{2}\rho_{\ell 0}' U_0'^2}, \qquad \mathrm{Re}(T_R) = \frac{\rho_{\ell 0}' U_0' R_0'}{\mu_\ell'(T_R')},$$

and

$$We(T_R) = \frac{\rho_{\ell 0}' U_0'^2 R_0'}{S'(T_R')} \tag{34}$$

and where $C_p(t)$ is the pressure coefficient given by

$$C_p(t) = \frac{p_0' - p_\infty'(t')}{\frac{1}{2}\rho_{\ell 0}' U_0'^2}, \tag{35}$$

with $p_\infty'(t')$ denoting the driving acoustic pressure. Furthermore, $p_0'$ is the reference background pressure, $U_0' = R_0'/\Theta'$ is a typical speed for normalization, $p_{v,sat}'(T_R')$ is the saturated vapor pressure at the bubble wall temperature, $S'(T_R')$ is the surface tension coefficient at the bubble wall temperature, and $\mu_\ell'(T_R')$ is the liquid viscosity at the bubble wall temperature. The normalized Keller–Miksis equation (33) can be employed only when the wall Mach number remains sufficiently small. Before applying the above acoustic cavitation model based on the novel gas pressure law, given by Eqs. (19) and (20), to single acoustic cavitation bubbles, we wish to discuss estimates of the function $f(Pe, \vartheta)$ entering the model through the novel gas pressure law.

## V. ESTIMATES OF THE FUNCTION $f(Pe, \vartheta)$

In this section, we identify the function $f(Pe, \vartheta)$ for small amplitude oscillations of the acoustic bubble by utilizing the well-established linear theory, and we attempt to obtain its estimates for large amplitude oscillations by the numerical simulations of Eqs. (1)–(3) with appropriate initial and boundary conditions.

### A. Identification of the function $f(Pe, \vartheta)$ for small amplitude oscillations

For small amplitude oscillations of the bubble, the normalized bubble wall temperature $T_R$, which enters the novel reduced order gas pressure law given by Eq. (19), can be taken to be unity so that the reduced order gas pressure law reduces to the polytropic gas law with the polytropic index $\Gamma$ given by Eq. (20). In this case, the normalization time scale $\Theta'$ can be identified as the reciprocal of the forcing frequency $\omega'$ so that the Péclet number $Pe$, given by Eq. (2), takes the form

$$Pe = \frac{R_0'^2\,\omega'}{\alpha_g'}, \tag{36}$$

where $\alpha_g'$ is the thermal diffusivity of the gas. Furthermore, by solving from Eq. (20) for the function $f$ in terms of the isentropic index $\gamma$ and the polytropic index $\Gamma$, we arrive at

$$f = \frac{(3\gamma - 1)\,\Gamma - 2\gamma}{2\,(\gamma - \Gamma)}, \tag{37}$$

where the polytropic index $\Gamma$, in general, depends on the Péclet number $Pe$ and the normalized characteristic time $\vartheta$. It can readily be seen that in the isothermal limit as $\Gamma \to 1$, $f(Pe, \vartheta) \to 1/2$ and in the adiabatic limit as $\Gamma \to \gamma$, $f(Pe, \vartheta) \to \infty$, as demonstrated before. The solution of small amplitude oscillations of a single bubble under an acoustic pressure signal is well-known. Devin,[24] following Pfriem,[25] considered the thermal damping of an acoustic bubble in the uniform pressure approximation near resonance using the polytropic expansion and compression of the gas. Under these conditions, he related the polytropic index $\Gamma$ to the Péclet number $Pe$ throughout the relation

$$\Gamma = \gamma\,(2\,Pe)^{3/2}\,\frac{[\,(2\,Pe)^{1/2} + 3\,(\gamma - 1)\,\mathcal{A}_-\,]}{(2\,Pe)\,[(2\,Pe)^{1/2} + 3\,(\gamma - 1)\,\mathcal{A}_-]^2 \;+\; 9\,(\gamma - 1)^2\,[(2\,Pe)^{1/2}\,\mathcal{A}_+ - 2]^2}, \tag{38}$$

where $\mathcal{A}_\pm$ is given by

$$\mathcal{A}_\pm = \frac{\sinh(\sqrt{2\,Pe}) \;\pm\; \sin(\sqrt{2\,Pe})}{\cosh(\sqrt{2\,Pe}) - \cos(\sqrt{2\,Pe})}. \tag{39}$$

In this case, the forcing angular frequency $\omega'$ in Eq. (36) for the Péclet number is replaced by the surface tension-free Minnaert frequency $\omega_M'$. The resonance frequency $\omega_0'$ then deviates from the Minnaert frequency $\omega_M'$ due to the inclusion of thermal damping and, possibly, of surface tension (for details, see Leighton[3] and Prosperetti[26]). The corresponding thermal damping coefficient can also be found in the references therein and is shown to vanish in both of the cases as $Pe \to 0$ (the isothermal case, $\Gamma \to 1$ or $f \to 1/2$) and $Pe \to \infty$ (the adiabatic case, $\Gamma \to \gamma$ or $f \to \infty$), showing a maximum in between. Eller[27] extended Devin's work under the same assumptions for the damping of bubbles driven by off-resonance frequencies and found the same expression (38) for the polytropic index $\Gamma$. Prosperetti[28] presented a general linearized theory of small amplitude pulsations of a bubble, allowing for pressure variations within the bubble where he describes the thermal effects in terms of a polytropic index and a thermal damping coefficient. His results for the polytropic index showed dependence on the gas parameters $G_1$ and $G_2$, where $G_1 = \omega'/(c_g'/\ell')$ (a normalized time scale) is the ratio of the forced angular frequency to the mean collision frequency of the gas molecules. with $c_g'$ denoting the speed of sound in the gas and $\ell'$ denoting the mean free path of the gas molecules, and where $G_2$ is precisely the Péclet number given by Eq. (36). In particular, Prosperetti showed, when $(G_1\,G_2)^{1/2}$ is sufficiently small, the

uniform pressure approximation within the bubble holds, and the polytropic index given by Prosperetti[28] (depending on $G_1$ and the Péclet number) becomes the polytropic index Γ previously given for small amplitude oscillations. Results for the polytropic index Γ as a function of $G_2$ (the Péclet number) with different values of $G_1$ can be found in various studies[3,28] for different values of the isentropic exponent $\gamma$. Furthermore, Crum[29] showed that Prosperetti's formulation for the polytropic index reduces to that given by Devin[24] and Eller[27] [Eqs. (38) and (39)] under the same assumptions in the uniform pressure approximation. It should be emphasized that Prosperetti's results of small amplitude bubble pulsations are more general as they apply at high insonation frequencies where pressure nonuniformities become important. Except for high insonation frequencies, we have shown how the present formulation recovers the small amplitude pulsation results by identifying the polytropic index Γ (and thus the function $f$) as a function of the Péclet number $Pe = G_2$.

### B. Estimates of the function $f(Pe, \vartheta)$ for large amplitude oscillations

We now consider the numerical solution of the original system of partial/ordinary differential equations for large amplitude oscillations of a single gas bubble in the uniform pressure approximation and compare the results against those obtained by the reduced order gas pressure law in order to obtain estimates of the function $f$ corresponding to particular Péclet numbers and characteristic times. Before we proceed, we would like to obtain estimates of $f$ in the nearly isothermal case, where an asymptotic expression for the gas pressure is available from the near isothermal model of Prosperetti.[12] In this model, the original equations (1) and (3) are solved asymptotically by carrying out regular perturbation expansions of the Péclet number for the temperature and pressure inside the bubble but using prescribed values for the bubble radius. Consequently, the equation for the gas pressure, to $O(Pe)$, takes the simple form

$$\frac{p}{p_{g0}} = \frac{1}{R^3}\left[1 - \frac{(\gamma-1)\,(Pe)}{5\,\gamma}\,\frac{\dot{R}}{R^2}\right]. \tag{40}$$

In Eq. (40), the $O(1)$ term of the gas pressure is the isothermal gas pressure law, where the prescribed radius can be obtained from the isothermal solution of the Keller–Miksis equation (33). If, in addition to the gas pressure and temperature perturbation expansions, a regular perturbation expansion of the Péclet number for the bubble radius $R$ was carried out in the solution of Eqs. (1) and (3) together with the Keller–Miksis equation, we would arrive at the gas pressure expression (the consistent near isothermal expression)

$$\frac{p}{p_{g0}} = \frac{1}{R_{is}^3}\left\{1 - (Pe)\left[\frac{(\gamma-1)}{5\,\gamma}\,\frac{\dot{R}_{is}}{R_{is}^2} + 3\,\frac{R_1}{R_{is}}\right]\right\}, \tag{41}$$

where $R_{is}$ is the isothermal bubble radius and $R_1$ is the bubble radius contribution in the $O(Pe)$ term of the bubble perturbation expansion (for details, see Appendix B). In particular, $R_{is}$ is obtained from the isothermal solution of the Keller–Miksis equation (B15), and $R_1$ is obtained from the solution of the linear equation (B16) given in Appendix B. A typical validation of the above near isothermal gas pressure expression given by Prosperetti[12] against full computations using a spectral collocation method based on orthogonal Chebyshev polynomials has already been carried out by Preston.[38] We here compare the solutions of the reduced order gas pressure law given by Eqs. (19) and (20) with the gas pressure expression (40) given by

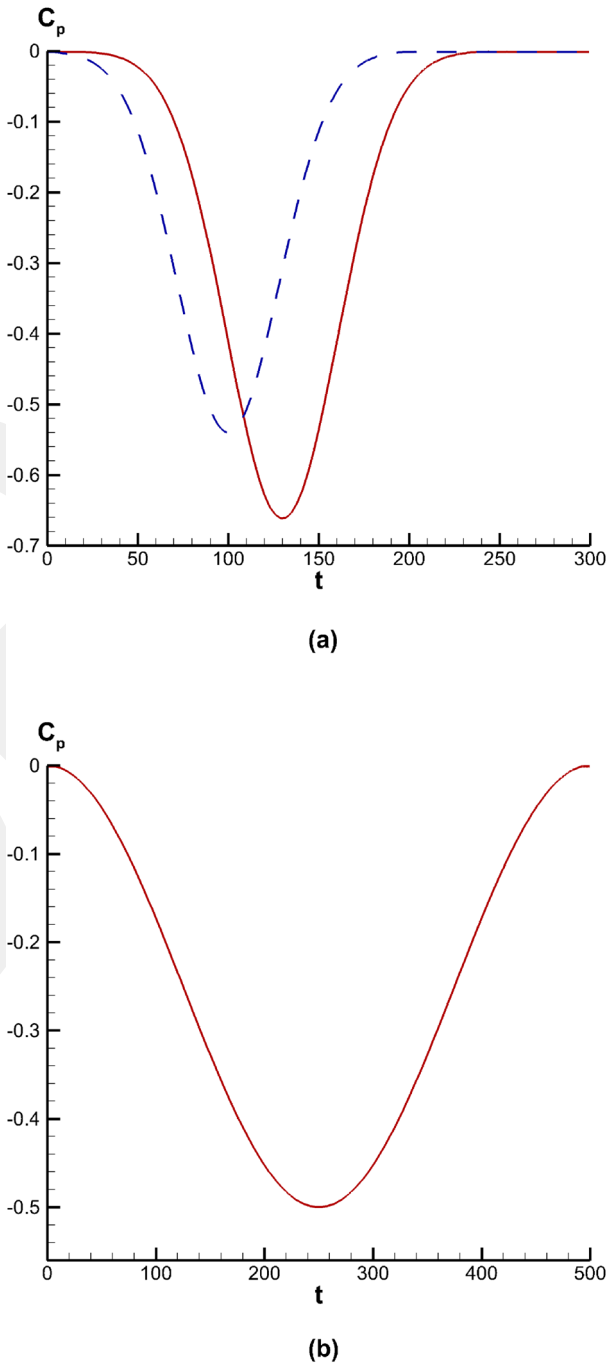


**FIG. 2.** (a) Time variations of the pressure signal coefficients given, respectively, by Eq. (42) (dashed line) and Eq. (56) (solid line). (b) Variation of the pressure signal coefficient given by Eq. (57) with respect to normalized time.

Prosperetti and with the consistent near isothermal expression (41) carried out in Appendix B using the Keller–Miksis equation (33) for spherical bubble dynamics under the same driving acoustic pressure signal,

$$C_p(t) = -0.54\ \exp\left[-\left(\frac{t-100}{40}\right)^2\right],\quad 0 < t < 300, \tag{42}$$

plotted in Fig. 2(a) for an air bubble with initial equilibrium radius $R_0' = 40\ \mu$m in water at 25 °C. For the numerical computations by the fifth order Runge–Kutta–Fehlberg method, we use the normalization time $\Theta' = 2.0 \times 10^{-7}$ s corresponding to the Péclet number $Pe = 3.55$. The results of the temporal variations of the normalized bubble radius and gas pressure obtained by the near isothermal gas pressure solution of Prosperetti by the consistent near isothermal solution and by the novel gas pressure law for $f = 0.6$ [the value obtained from the linear theory of Eqs. (37)–(39)] using the Keller–Miksis equation of spherical bubble dynamics are plotted in Figs. 3(a) and 3(b). Excellent agreement is achieved, with almost no differences, for the temporal variations of the normalized bubble radius and of the normalized gas pressure between those of the present model and the near isothermal Prosperetti model, whereas relatively small deviations arise in the results of the consistent near isothermal model. It seems that the value of the parameter $f$ for relatively low Péclet numbers (near isothermal change of state) can be approximated by the value obtained from Eqs. (37)–(39) of the linear theory, provided that the computational time scale $\Theta'$ is used in the definition of the Péclet number instead of the reciprocal of the Minnaert frequency.

We now return to the full numerical solution of the system of equations [(1) and (3)] subject to the initial and boundary conditions given by Eq. (4) to obtain estimates of the function $f(Pe, \vartheta)$. For simplicity, we use the boundary condition $T(t,1) = T_R(t) = 1$ so that the temperature distribution within the thin liquid boundary layer becomes uniform [$T_\ell(t,y) = 1$ for $y > 1$]. This avoids the use of the energy equation (22) in the surrounding liquid and simplifies the reduced order gas pressure law to that given by Eq. (21). By eliminating $dp/dt$ between Eqs. (1) and (3), we can write the energy equation in the bubble interior as

$$\frac{\partial T}{\partial t} = \frac{1}{(Pe)\,p\,R^2}\left\{\left[3(\gamma-1)\,T + y\,\frac{\partial T}{\partial y}\right]\left(\frac{\partial T}{\partial y}\right)_{y=1^-} + \left(\frac{2}{y}\,T - \frac{\partial T}{\partial y}\right)\frac{\partial T}{\partial y} + T\,\frac{\partial^2 T}{\partial y^2}\right\} - \frac{3(\gamma-1)}{R}\,\frac{dR}{dt}\,T \tag{43}$$

coupled to Eq. (3) for the gas pressure and to the Keller–Miksis equation (33) for spherical bubble dynamics. The boundary conditions for Eq. (43) become

$$T(t, y = 1^-) = 1 \quad \text{and} \quad \left(\frac{\partial T}{\partial y}\right)_{y=0} = 0. \tag{44}$$

We use the spectral method to reduce the energy partial differential equation (43), subject to the boundary conditions (44) and coupled to the ordinary differential equations (3) and (33) for the gas pressure and for the bubble radius, to a system of ordinary differential equations. For this reason, we expand the temperature field

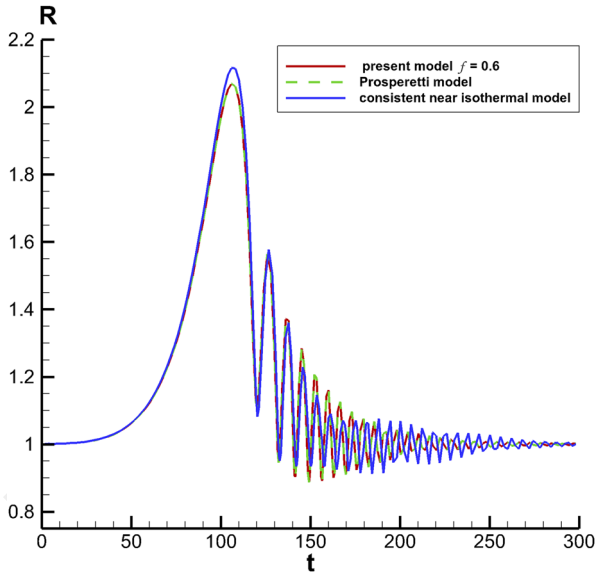


(a)

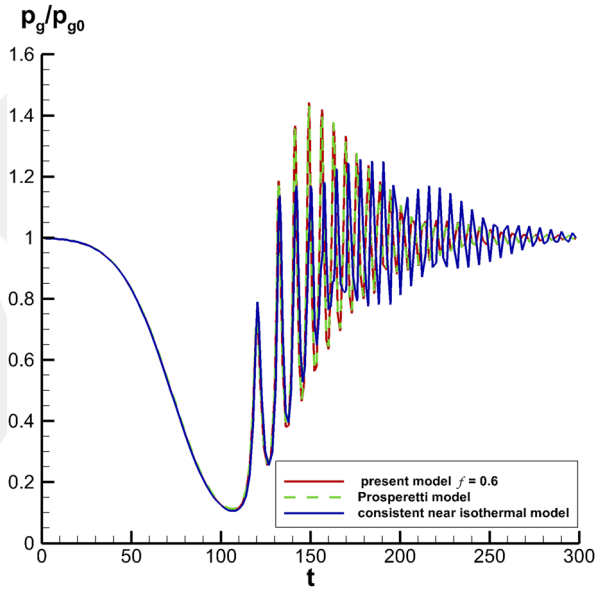


(b)

**FIG. 3.** (a) Comparison of the temporal evolution of the normalized bubble radius driven by the acoustic pressure given by Eq. (42) for an air bubble in water with the initial equilibrium radius $R_0' = 40\ \mu$m, the Weber number $We(1) = 166$, the Reynolds number $Re(1) = 780$, and the Péclet number $Pe = 3.55$ using the present reduced order gas pressure law given by Eq. (21) for $f = 0.6$, the near isothermal solution of Prosperetti[12] given by Eq. (40), and the consistent near isothermal solution given by Eq. (41). (b) Comparison of the temporal evolution of the normalized gas pressure under the conditions stated in (a) using the present reduced order gas pressure law given by Eq. (21) for $f = 0.6$, the near isothermal solution of Prosperetti[12] given by Eq. (40), and the consistent near isothermal solution given by Eq. (41).

$T(t,y)$ in terms of the orthogonal Chebyshev polynomials $\mathcal{T}_k(y)$ in the form[15,33]

$$T(t,y) = \sum_{k=0}^{N} a_k(t)\, \mathcal{T}_{2k}(y) \tag{45}$$

for sufficiently large $N$ where even orders of the Chebyshev polynomials are chosen to ensure that the boundary condition $(\partial T/\partial y)_{y=0} = 0$ at the bubble center is automatically satisfied. By substituting the relations,

$$\frac{\partial T}{\partial t} = \sum_{k=0}^{N} \dot{a}_k\, \mathcal{T}_{2k}(y), \tag{46}$$

$$\frac{\partial T}{\partial y} = \sum_{k=0}^{N} a_k(t)\, \frac{\partial \mathcal{T}_{2k}}{\partial y} = \sum_{k=0}^{N} \frac{2k\, \sin(2kz)}{\sin z}\, a_k(t), \tag{47}$$

and

$$\begin{aligned}\frac{\partial^2 T}{\partial y^2} &= \sum_{k=0}^{N} a_k(t)\, \frac{\partial^2 \mathcal{T}_{2k}}{\partial y^2} \\ &= \sum_{k=0}^{N} \frac{2k\,[\cos z\, \sin(2kz) - 2k \sin z\, \cos(2kz)]}{\sin^3 z}\, a_k(t),\end{aligned} \tag{48}$$

where $z = \arccos(y)$ into Eq. (43), we arrive at a system of first order ODEs for the time dependent coefficients $a_k(t)$,

$$\begin{aligned}\dot{a}_k = \frac{1}{(Pe)\, p\, R^2} \Bigg\{ & \left[ 12(\gamma - 1) + \frac{8k\, y\, \sin(2kz)}{\sin z\, \mathcal{T}_{2k}(y)} \right] \left( \sum_{\ell=0}^{N} \ell^2\, a_\ell \right) \\ & + \left[ \frac{4}{y} - \frac{4k\, \sin(2kz)}{(\sin z)\, \mathcal{T}_{2k}(y)} \right] \left( \sum_{\ell=0}^{N} \frac{\ell\, \sin(2\ell z)}{\sin z}\, a_\ell \right) \\ & + \sum_{\ell=0}^{N} \frac{(2\ell)[\cos z\, \sin(2\ell z) - 2\,\ell \sin z\, \cos(2\ell z)]}{\sin^3 z} \\ & \times a_\ell - 3\,(\gamma - 1)\,(Pe)\, p\, R\, \dot{R} \Bigg\}\, a_k\end{aligned} \tag{49}$$

for $k = 0, 1, 2, \ldots, N$ and fixed $y$. The boundary condition $T(t,1) = 1$ now becomes

$$\sum_{k=0}^{N} a_k(t) = 1. \tag{50}$$

Equations (3) and (49) together with (47) at the bubble wall ($y = 1$) and the Keller–Miksis equation (33) for spherical bubble dynamics with specified initial radius and initial radius velocity then form an initial value problem (IVP) for the bubble radius $R(t)$, the uniform gas pressure $p(t)$, and the temperature field $T(t,y); 0 < y < 1$ and can be solved by conventional Runge–Kutta methods. The results of the pressure and temperature fields using full numerical simulations of the underlying fundamental equations in the uniform pressure approximation under similar conditions by the proper orthogonal decomposition method are already available.[38] The velocity field in the uniform pressure approximation can then be obtained by the well-known exact formula[11] using the solutions of the bubble radius, the pressure field, and the temperature field. For the validation of the reduced order gas pressure law, we only need to consider the system of ODEs for $a_k(t)$ at the bubble wall ($y = 1$), which reduces to

$$\begin{aligned}\dot{a}_k = \frac{1}{(Pe)\, p\, R^2} \Bigg\{ & 4\,(3\gamma - 1) \left[ N^2\,(1 - a_0) - \sum_{\ell=1}^{N-1} (N^2 - \ell^2)\, a_\ell \right] \\ & + \frac{4}{3} \Bigg[ N^2\,(4N^2 - 1)\,(1 - a_0) \\ & - \sum_{\ell=1}^{N-1} \left( N^2(4N^2 - 1) - \ell^2(4\ell^2 - 1) \right) a_\ell \Bigg] \\ & - 3\,(\gamma - 1)\,(Pe)\, p\, R\, \dot{R} \Bigg\}\, a_k\end{aligned} \tag{51}$$

for $k = 0, 1, 2, \ldots, N-1$ since $a_N(t) = 1 - \sum_{k=0}^{N-1} a_k(t)$. Using Eq. (47) for the temperature gradient at the bubble wall ($y = 1$), the ODE for the gas pressure given by Eq. (3) becomes

$$\dot{p} = \frac{3\gamma}{(Pe)\, R^2} \left[ 4\, N^2\,(1 - a_0) - 4 \sum_{\ell=1}^{N-1} (N^2 - \ell^2)\, a_\ell - (Pe)\, p\, R\, \dot{R} \right]. \tag{52}$$

Moreover, in order to be able to consider the initial value problem of the system of ODEs given by Eqs. (51) and (52) coupled to the Keller–Miksis equation (33), we need to specify initial conditions for the spherically symmetric temperature distribution as well as for the pressure and for the bubble radius together with the bubble wall velocity. For the spherically symmetric initial temperature distribution, we here assume a uniform isothermal temperature distribution $T(0,y) = \sum_{k=0}^{N} a_k(0)\, \mathcal{T}_{2k}(y) = 1$ for sufficiently large $N$. Using orthogonality relations of the even order Chebyshev polynomials on (0,1), we obtain the initial values for the coefficients $a_k(t); k = 0, 1, 2, 3, \ldots, (N-1)$ as

$$a_0(0) = 1 \qquad \text{and} \qquad a_k(0) = 0 \quad \text{for} \quad k = 1, 2, 3, \ldots, (N-1) \tag{53}$$

for the system of ODEs given by Eq. (51). It then follows from the boundary condition at the bubble wall that $a_N(0) = 0$. The initial conditions for the gas pressure and for the bubble radius together with the bubble wall velocity can be taken as

$$p(0) = p_{g0} \qquad \text{and} \qquad R(0) = 1\,, \ \dot{R}(0) = 0 \tag{54}$$

for a bubble in equilibrium where the initial equilibrium gas pressure $p_{g0}$ is obtained from the mechanical equilibrium condition (Laplace's equation). The nonlinear system of $N+3$ first order ordinary differential equations (51) and (52) together with the Keller–Miksis equation (33) subject to the initial conditions given by Eqs. (53) and (54) constitute an initial value problem (IVP) for the coefficients $a_k(t); k = 0, 1, 2, 3, \ldots, (N-1)$, the normalized uniform gas pressure $p(t)$, the bubble radius $R(t)$, and the bubble wall velocity $\dot{R}(t)$. The initial value problem for this system is solved using the 4/5 order Runge–Kutta–Fehlberg method with adaptive step size. An estimate of $f(Pe, \vartheta)$ for a fixed Péclet number $Pe$ can, in principle, be obtained by first evaluating the function $H(t; Pe)$, given by

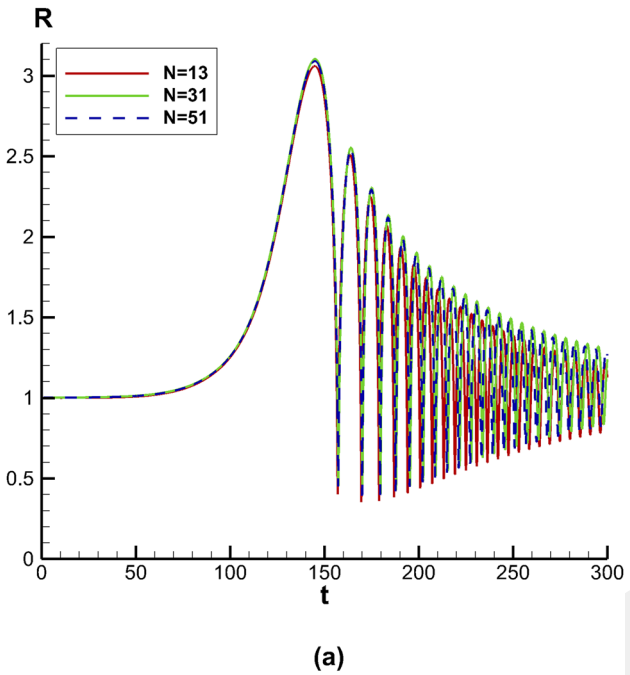


**FIG. 4.** (a) The temporal evolution of the normalized bubble radius driven by the acoustic pressure given by Eq. (56) for an air bubble in water with initial equilibrium radius $R_0' = 40\ \mu\mathrm{m}$, Weber number $We(1) = 166$, Reynolds number $Re(1) = 780$, Péclet number $Pe = 31.5$ using the numerical simulation of the original energy balance equations (1) and (3) for $N = 13, 31$, and 51 demonstrating the convergence of the solutions. (b) The temporal evolution of the normalized gas pressure of the air bubble in water under the conditions stated in (a) using the numerical simulation of the original energy balance equations (1) and (3) for $N = 13, 31$, and 51 demonstrating the convergence of the solutions.

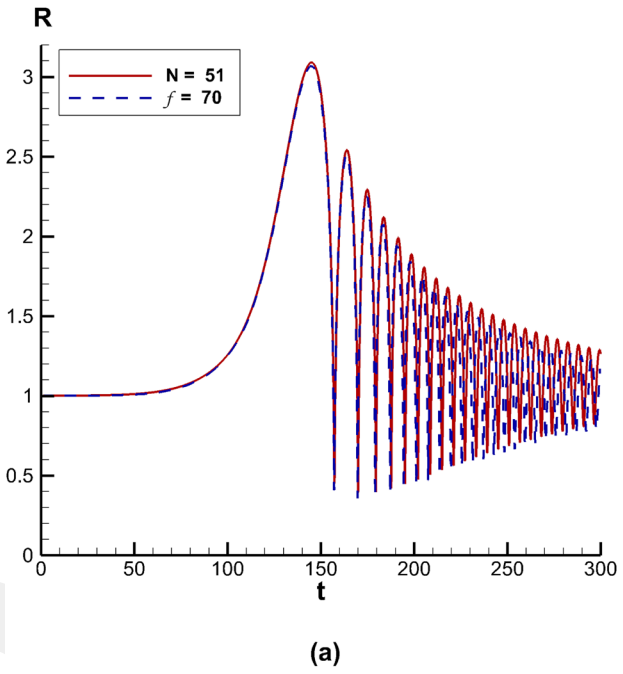


**FIG. 5.** (a) Comparison of the results of the temporal evolution of the normalized bubble radius driven by the acoustic pressure given by Eq. (56) for an air bubble in water under the conditions stated in Fig. 4 using the numerical simulation of the original energy balance equations (1) and (3) for $N = 51$ and the novel reduced order gas pressure law given by Eq. (21) for $f = 70$. (b) Comparison of the temporal evolution of the normalized gas pressure of the air bubble in water under the conditions stated in Fig. 4 using the numerical simulation of the original energy balance equations (1) and (3) for $N = 51$ and the novel reduced order gas pressure law given by Eq. (21) for $f = 70$.

$$H(t;Pe) = \frac{1}{2}\frac{\left(\frac{\partial^2 T}{\partial y^2}\right)_{y=1^-}}{\left(\frac{\partial T}{\partial y}\right)_{y=1^-}} = \frac{1}{6}\frac{\sum_{k=1}^{N} k^2\,(4\,k^2-1)\,a_k(t)}{\sum_{k=1}^{N} k^2\,a_k(t)} \tag{55}$$

from the numerical solution of the coefficients $a_k(t); k = 0, 1, 2, 3, \ldots, (N-1)$, where the Péclet number dependence is implicit, together with the relation $a_N(t) = 1 - \sum_{k=0}^{N-1} a_k(t)$. We then use Eq. (17) to get an average of this function by integrating it over a computational normalized characteristic time $\vartheta$. For a typical example, we consider the acoustic excitation of an air bubble with initial equilibrium radius $R_0' = 40\ \mu$m in water at $T_0' = 25\,^\circ$C by the acoustic pressure signal

$$C_p(t) = -0.662\ \exp\left[-\left(\frac{t-130}{43.5}\right)^2\right],\quad 0 < t < 300, \tag{56}$$

shown in Fig. 2(a) corresponding to the Reynolds number $Re = 780$, the Weber number $We = 166$, and the Péclet number $Pe = 31.5$. The results of the time evolution of the normalized bubble radius and that of the normalized gas pressure using the 4/5 order Runge–Kutta–Fehlberg method with adaptive time step for different values of $N$ ($N = 13, 31$, and 51) are plotted in Figs. 4(a) and 4(b), respectively. As can clearly be seen, the convergence of the solution is reached for $N = 51$. Considerable differences are observed between the temporal variations of the normalized bubble radius and, particularly, those of the normalized gas pressure for the cases $N = 13$ and $N = 51$, whereas the differences seem to be reduced for the cases $N = 31$ and $N = 51$. Now, the value of $f$ can, in principle, be estimated from the numerical simulations during the first collapse of the bubble. Unfortunately, the function $H(t;Pe)$ varies by orders of magnitude during this period, especially during violent collapses of ultrashort duration. Therefore, we find it more convenient to find the best value of $f$ that fits the numerical simulations [in this case, the value of $f$ obtained by Eqs. (37)–(39) from the linear theory is far off from that of the best fit]. The results of the numerical simulations for the temporal variations of the normalized bubble radius and of the normalized gas pressure together with those using the reduced order gas pressure law for $f = 70$ are plotted in Figs. 5(a) and 5(b). Good agreement is observed between the time variations of the normalized bubble radius obtained by the numerical simulations and those obtained using the novel gas pressure law for $f = 70$, as well as between the time variations of the normalized gas pressure for both cases, verifying the validity of the novel gas pressure law.

## VI. RESULTS FOR ACOUSTIC CAVITATION

In this section, we present results of the above acoustic cavitation model using the reduced order gas pressure law of Secs. II and IV. For this reason, we first employ the Keller–Miksis equation (33) where the reduced order gas pressure law is incorporated by varying $f$, corresponding to different Péclet numbers and characteristic time scales, together with the Plesset–Zwick equation (31) for the bubble wall temperature $T_R$. We then compare the results obtained with those where the gas pressure is given by the adiabatic ($f \to \infty$) or by the isothermal law ($f = 1/2$ and $T_R = 1$). For the numerical solution, we use the 4/5 order Runge–Kutta–Fehlberg method to solve the initial value problem of the Keller–Miksis equation (33) and Simpson's 3/8-rule of numerical integration to integrate the Plesset–Zwick equation (31).

We consider the acoustic cavitation of water–vapor/air bubbles in water using two different driving acoustic pressure signals, one previously given by Eq. (56) [14] and the other given by Wang,[39] whose pressure coefficient is

$$C_p(t) = -0.25\left[1 - \cos\left(\frac{2\pi t}{500}\right)\right],\quad 0 < t < 500, \tag{57}$$

as shown in Fig. 2(b). For the Preston *et al.* acoustic pressure signal given by Eq. (56), we choose the initial equilibrium bubble radius to be $R_0' = 40\ \mu$m, the bulk water temperature to be at $T_0' = 25\,^\circ$C with saturated vapor pressure $p_{v0}' = 0.0316$ bar, surface tension coefficient $S' = 0.0720$ N/m, and viscosity of water $\mu_{\ell 0}' = 8.9 \times 10^{-4}$ kg/m s, and for the Wang acoustic pressure signal given by Eq. (57), we choose the initial equilibrium bubble radius to be $R_0' = 100\ \mu$m, the bulk water temperature to be at $T_0' = 20\,^\circ$C with saturated vapor pressure $p_{v0}' = 0.0233$ bar, surface tension coefficient $S' = 0.0728$ N/m, and viscosity of water $\mu_{\ell 0}' = 10^{-3}$ kg/m s. In both cases, the normalized computational time is chosen to be $\Theta' = 2.3\ \mu$s. For these cases, the initial nondimensional parameters entering the computations are $\sigma(1) = 0.656$, $Re(1) = 780$, $We(1) = 166$, and $Pe = 31.83$ for the Preston *et al.* acoustic pressure signal and $\sigma(1) = 0.492$, $Re(1) = 1000$, $We(1) = 137$, and $Pe = 12.37$ for the Wang acoustic pressure signal. For both acoustic pressure signals, we present results where the interface properties are taken constant at the bulk liquid temperature ($T_R = 1$) as well as results where the interface properties vary with temperature $T_R$ given by the Plesset–Zwick solution.

Figure 6 shows the variation of the normalized radius $R$ and the normalized wall temperature $T_R$ against the normalized time $t$ for different values of $f$ ($f = 0.5$, 1, and 10 corresponding to different Péclet numbers) of the Preston *et al.* acoustic pressure signal using the present acoustic cavitation model with constant interface properties at the bulk liquid temperature under the conditions stated above. The plots show that the variation of the bubble radius lies between the adiabatic and isothermal change of state of the gas for different values of $f$. However, the variations of the bubble wall temperatures during bubble collapse vary by orders of magnitude exceeding the critical value ($T_R = 2.17$), which implies that interface properties cannot be taken as constants. Actually, the calculated bubble wall temperatures are far off in magnitude from the maximum wall temperatures ($T_R \sim 1.2$) obtained by the full computations of the model equations of Preston *et al.*[14] This suggests that interface properties varying with bubble wall temperature should be used. These properties for air–water vapor bubbles in water are summarized in Appendix B. Figure 6 shows the variation of the normalized radius $R$ and the normalized wall temperature $T_R$ against the normalized time $t$ for different values of $f$ ($f = 0.5$, 1, and 10) by the present acoustic model but using variable properties at the interface under the same conditions. Considerable differences are observed between the results of both the normalized radius and the bubble wall temperature temporal variations presented in Fig. 6 for constant interface properties and in Fig. 7 for variable interface properties.

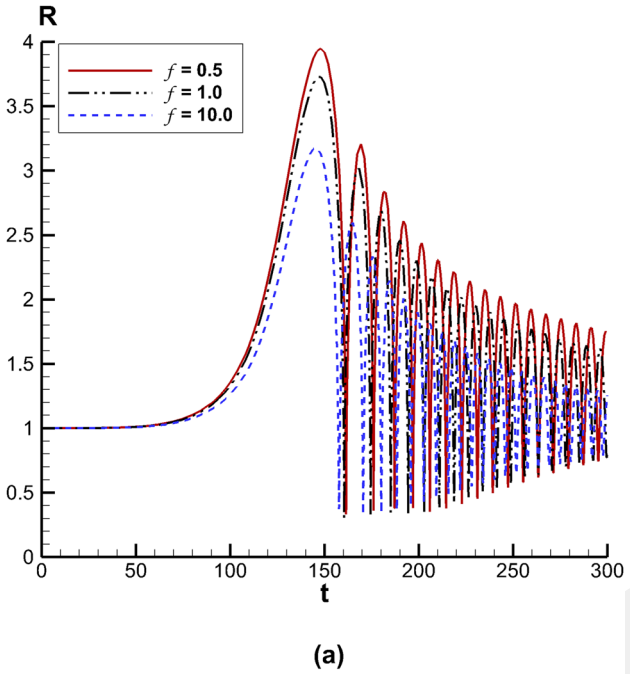


**FIG. 6.** (a) The temporal evolution of the normalized bubble radius driven by the acoustic pressure given by Eq. (56) for an air–water vapor bubble in water with the initial equilibrium radius $R_0' = 40\ \mu\mathrm{m}$, initial cavitation number $\sigma(1) = 0.656$, Weber number $We(1) = 166$, and Reynolds number $Re(1) = 780$ using constant interface properties by the present acoustic cavitation model for different values of $f$ ($f$ = 0.5, 1, and 10). (b): The temporal evolution of the normalized bubble wall temperature of the air–water vapor bubble in water under the conditions stated in (a) by the present acoustic cavitation model for different values of $f$ ($f$ = 0.5, 1, and 10).

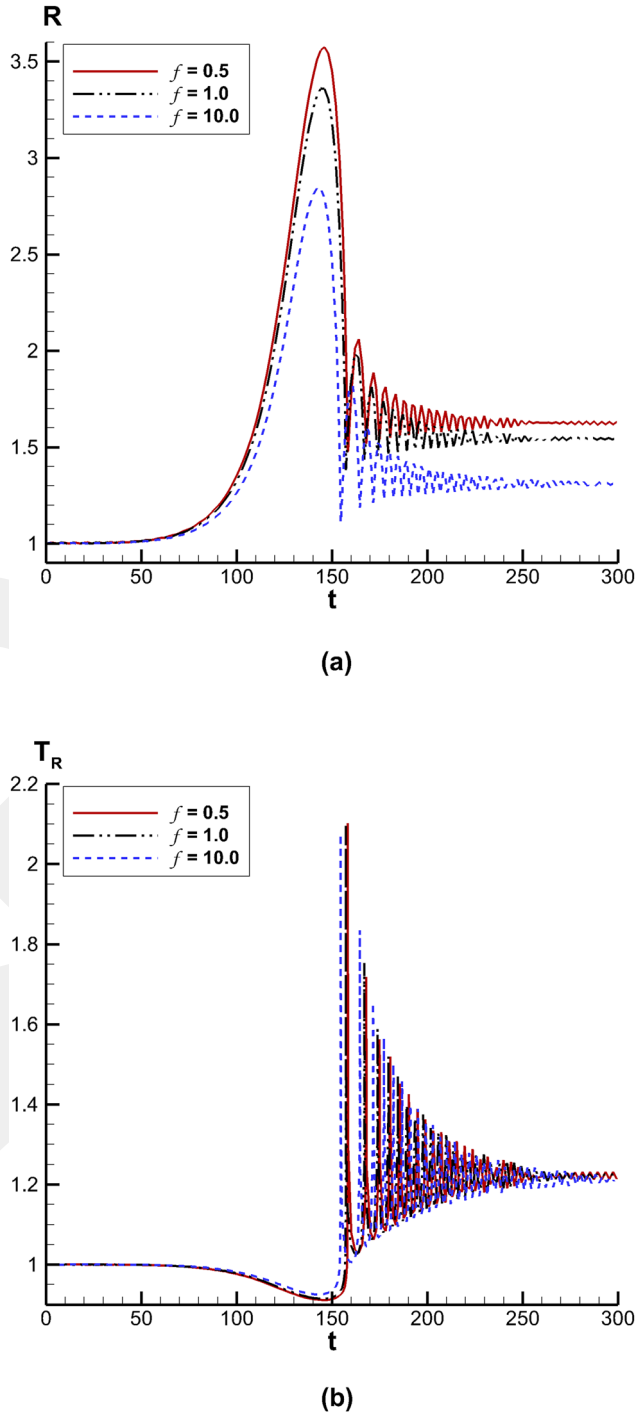


**FIG. 7.** (a) The temporal evolution of the normalized bubble radius driven by the acoustic pressure given by Eq. (56) for an air–water vapor bubble in water under the conditions stated in Fig. 6 by the present acoustic cavitation model for different values of $f$ ($f$ = 0.5, 1, and 10) using variable properties at the interface. (b) The temporal evolution of the normalized bubble wall temperature of the air–water vapor bubble in water under the conditions stated in Fig. 6 by the present acoustic cavitation model for different values of $f$ ($f$ = 0.5, 1 and 10) using variable properties at the interface.

The bubble radius amplitude variations are considerably reduced when variable interface properties are used for the same value of $f$, and the bubble radius is observed to tend rapidly to a new equilibrium at a value greater than that of the initial radius (different equilibrium values are reached for different values of $f$). More drastically, when variable interface properties are used, the bubble wall temperature variations in this case are reduced by an order of magnitude tending almost to the same equilibrium value ($T_R \sim 1.2$) for different values of $f$. We also compare the results of the present model with those of the constant mass transfer model of Preston *et al.*,[14] which agree well with the full computations of the governing equations under the same conditions. Before proceeding, however, we should note that the constant mass transfer model of Preston *et al.*[14] uses the classical Rayleigh–Plesset equation for incompressible fluid, whereas the present model lacks the mass diffusion effects both inside the bubble and through the liquid (infinitely fast mass diffusion case). Therefore, the comparison should be made keeping these details in mind. Figure 8(a) shows a comparison between the results of the temporal variations of the bubble radius obtained by the constant transfer model of Preston *et al.* for infinitely fast mass diffusion and those obtained by the present acoustic cavitation model for $f = 0.5$ using the Rayleigh–Plesset equation and constant interface properties. The bubble radius amplitudes of the present acoustic model seem to be smaller during initial growth and subsequent rebounds, except for times to the end of the cycle as compared to the constant transfer model with infinitely fast mass diffusion. In both cases, the initial growth and subsequent rebounds are overestimated as compared to full computations of the governing equations,[14] showing the importance of the finite mass diffusion effect. The results of the temporal variations of the bubble radius using the present acoustic cavitation model employing the Keller–Miksis equation for spherical bubble dynamics instead of the classical Rayleigh–Plesset equation are also plotted in Fig. 8(a), showing considerable reduction of the initial growth and subsequent rebounds of the bubble radius, which emphasizes the importance of the compressibility effects of the liquid. Figure 8(b) shows the same comparison between the results of the bubble radius temporal variations using the present acoustic cavitation model obtained using the Rayleigh–Plesset and the Keller–Miksis equation with variable interface properties and those obtained by Preston *et al.*[14] using the constant transfer model with infinitely fast mass diffusion. In this case, also considerable reduction in the initial growth and subsequent rebounds of the bubble radius is observed, exhibiting the importance of using variable properties in the proposed acoustic cavitation model.

Finally, we compare the results of the proposed acoustic cavitation model with those using the classical and isothermal laws in the Keller–Miksis equation for spherical bubble dynamics under the same conditions stated in Fig. 6. In this case, the comparison is made using constant interface properties at the bulk liquid temperature. We first compare the results for the classical adiabatic gas law and the proposed reduced order gas law for large values of the parameter $f$ ($f = 10^5$) using the Keller–Miksis equation. Figure 9(a) shows that the temporal evolution of the normalized radius agrees quite well in the first rebounds, whereas deviations are observed after the first a few rebounds. The comparison of the results for the temporal evolution of the bubble wall temperature using the classical adiabatic law and the Plesset–Zwick equation together with the

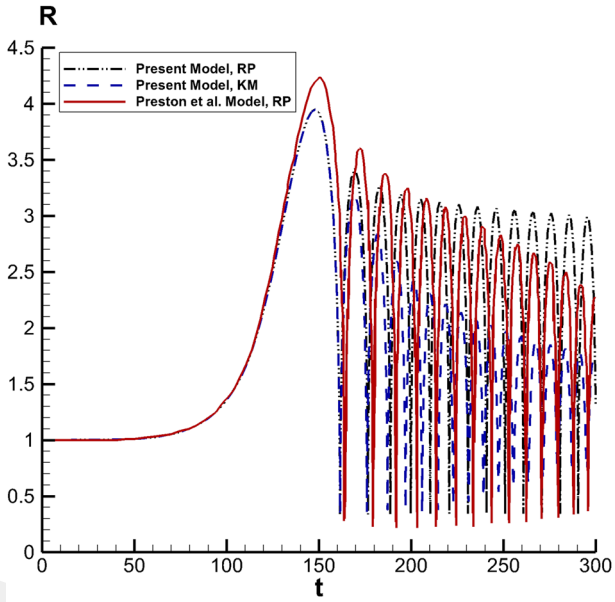


**FIG. 8.** (a) Comparison of the temporal evolution of the normalized bubble radius driven by the acoustic pressure given by Eq. (56) for an air–water vapor bubble in water under the conditions stated in Fig. 6 by the present acoustic cavitation model for $f = 0.5$ (RP: Rayleigh–Plesset equation, KM: Keller–Miksis equation) using interface properties at the bulk liquid temperature with that of Preston.[38] (b) Comparison of the temporal evolution of the normalized bubble radius driven by the acoustic pressure given by Eq. (56) for an air–water vapor bubble in water under the conditions stated in Fig. 6 by the present acoustic cavitation model for $f = 0.5$ (RP: Rayleigh–Plesset equation, KM: Keller–Miksis equation) using variable properties at the interface with that of Preston.[38]

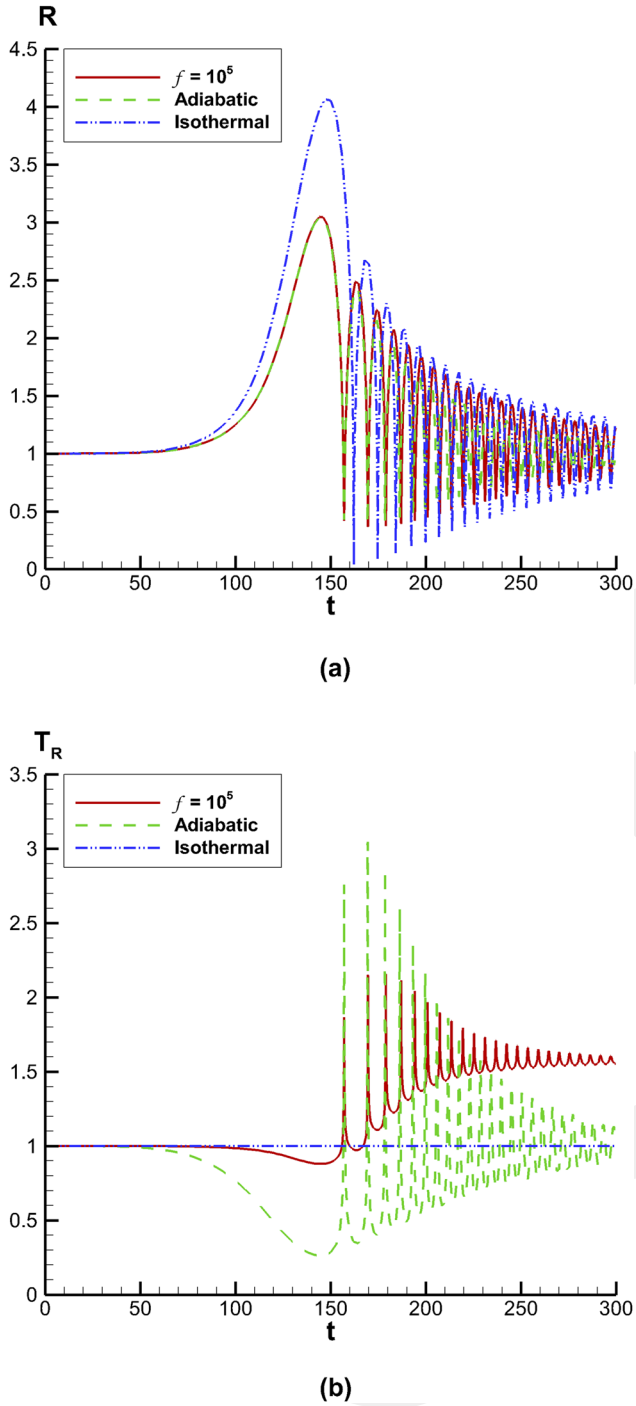


**FIG. 9.** (a) Comparison of the temporal evolution of the normalized bubble radius of the air–water vapor bubble in water under the conditions stated in Fig. 6 between results obtained by the Keller–Miksis equation (33) using the adiabatic gas law, the proposed acoustic model for $f = 10^5$, and the isothermal law. (b) Comparison of the temporal evolution of the bubble wall temperature of the air–water vapor bubble in water under the conditions stated in Fig. 6 between results obtained by the Keller–Miksis equation (33) using the adiabatic gas law, the proposed acoustic model for $f = 10^5$, and the isothermal law.

proposed model using large values of $f$ shows totally different behavior, as can be seen in Fig. 9(b). This shows that although the adiabatic pressure–radius relation is satisfied for large values of the parameter $f$ of the proposed model, the isentropic relations are not satisfied, showing that the perfect gas law is violated at the interface. The corresponding isothermal results, achieved when $f = 0.5$ and $T_R = 1$ in the absence of phase transition ($L \to 0$ as $T_R \to 1$) of the proposed acoustic model, are also shown in Fig. 9 for reference.

For the acoustic pressure signal given by Eq. (57),[39] the results for the temporal variations of the normalized bubble radius and of the normalized bubble wall temperature are plotted in Fig. 10 using the present acoustic cavitation model with constant interface properties (evaluated at the bulk liquid temperature) for different values of $f$ (0.5, 1, and 10). In this case, the maximum bubble radius of initial growth and the maximum bubble radii of the rebounds are seen to be reduced considerably as $f$ increases with increasing rebound frequencies. On the other hand, the bubble wall temperatures increased by an order of magnitude during collapse, invalidating the use of constant interfacial properties. As already demonstrated for the case of the driving acoustic pressure given by Eq. (56), the use of variable interfacial properties is essential in the present acoustic cavitation model. Figure 11 shows the results of the temporal behavior of the normalized bubble radius and of the normalized bubble wall temperature for the acoustic pressure signal given by Eq. (57) for the same values of $f$ (0.5, 1, and 10) but using variable interface properties. In this case, structural differences in the temporal variations of both the normalized bubble radius and the normalized bubble wall temperature are observed. The bubble grows initially in phase with the acoustic pressure attaining its maximum radius at the minimum value of the driving acoustic pressure and collapses to its initial equilibrium value with small amplitude local oscillations. Once again reduction in the maximum radius is observed as $f$ increases. The bubble wall temperature decreases in the bubble growth period, attains its minimum value at the minimum value of the driving acoustic pressure, and relaxes to its equilibrium value with small amplitude oscillations. Reduction in the minimum value is also observed as $f$ increases. The above results demonstrate the necessity of using variable properties at the interface in the present acoustic model. Finally, we compare the results of the temporal variations of the bubble radius and the bubble wall temperature obtained by the proposed acoustic cavitation model for large values of the parameter $f$ ($f = 10^5$) with those obtained using the classical adiabatic and isothermal gas laws. Figure 12(a) shows such a comparison of the bubble radius variations under the conditions stated in Fig. 10. In this case, excellent agreement is achieved between the results obtained by the classical adiabatic law and those obtained by the proposed acoustic cavitation model for $f = 10^5$ in the initial growth period and in the first a few rebounds of the bubble radius despite that slight differences appear after a few rebounds. Again considerable differences appear in the results of the temporal variations of the bubble wall temperature obtained by the classical isentropic relations and by the proposed acoustic cavitation model for large values of the parameter $f$ ($f = 10^5$), showing once again the violation of the ideal gas law at the interface. The corresponding isothermal results, achieved when $f = 0.5$ and $T_R = 1$ in the proposed acoustic model, are also shown for reference.

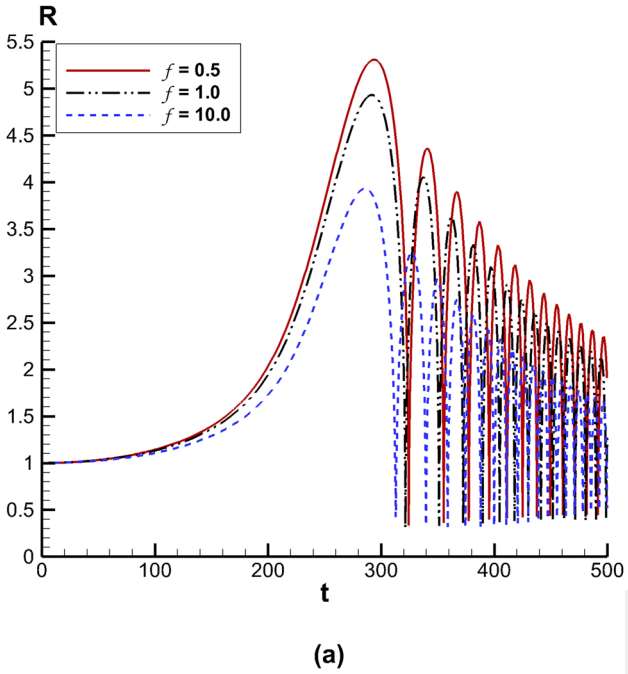


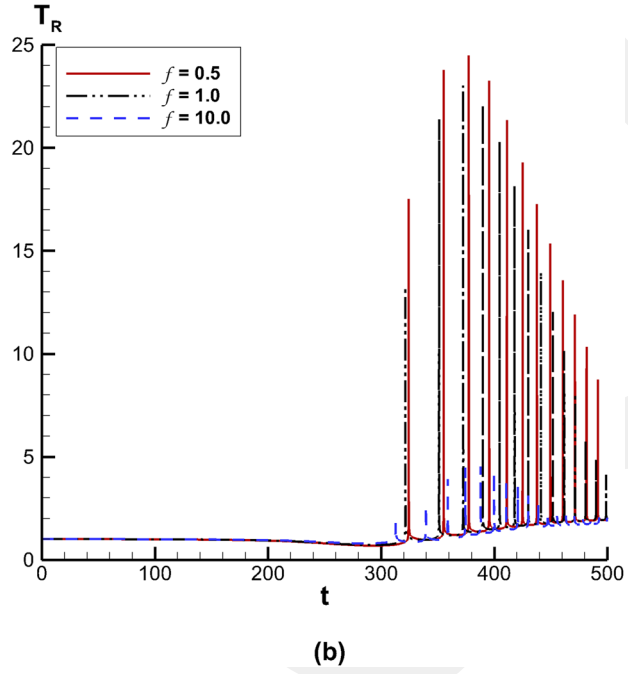


**FIG. 10.** (a) The temporal evolution of the normalized bubble radius driven by the acoustic pressure given by Eq. (57) for an air–water vapor bubble in water with the initial equilibrium radius $R_0' = 100\ \mu\mathrm{m}$, initial cavitation number $\sigma(1) = 0.492$, Weber number $We(1) = 137$, and Reynolds number $\mathrm{Re}(1) = 1000$ using constant interface properties by the present acoustic cavitation model for different values of $f$ ($f = 0.5$, 1, and 10). (b) The temporal evolution of the normalized bubble wall temperature of the air–water vapor bubble in water under the conditions stated in (a) by the present acoustic cavitation model for different values of $f$ ($f = 0.5$, 1, and 10).

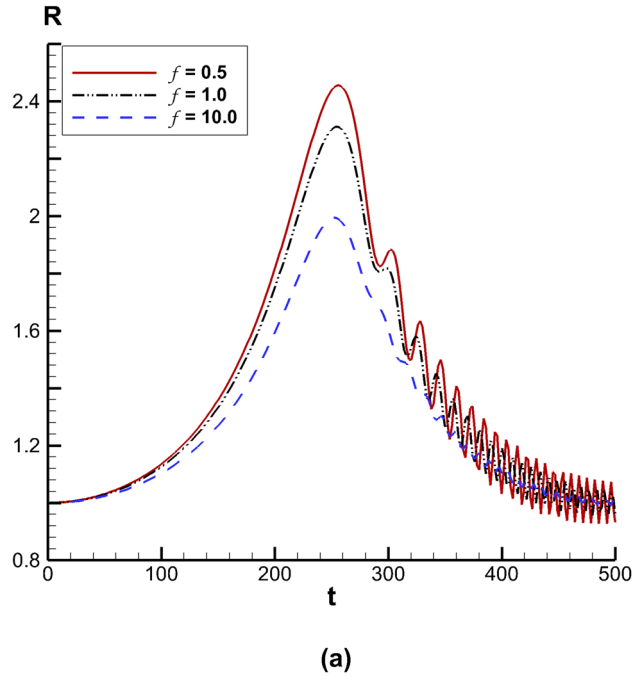


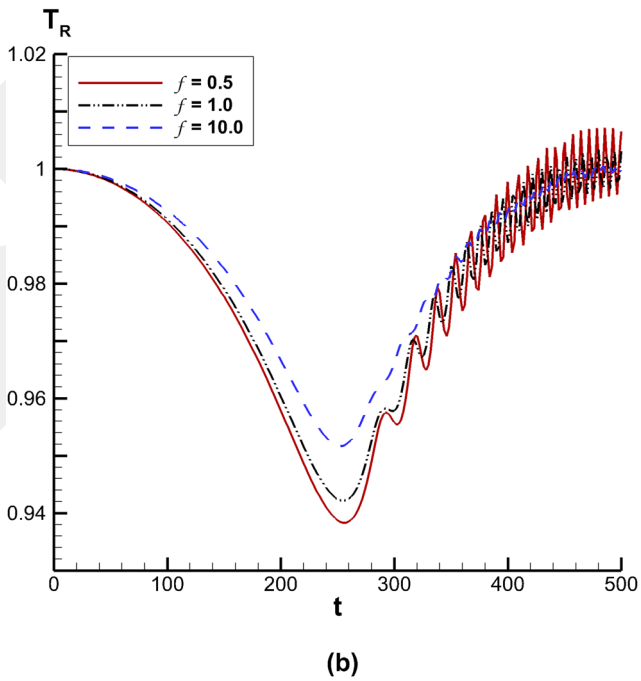


**FIG. 11.** (a) The temporal evolution of the normalized bubble radius driven by the acoustic pressure given by Eq. (57) for an air–water vapor bubble in water under the conditions stated in Fig. 10 by the present acoustic cavitation model for different values of $f$ ($f = 0.5$, 1, and 10) using variable properties at the interface. (b) The temporal evolution of the normalized bubble wall temperature of the air–water vapor bubble in water under the conditions stated in Fig. 10 by the present acoustic cavitation model for different values of $f$ ($f = 0.5$, 1, and 10) using variable properties at the interface.

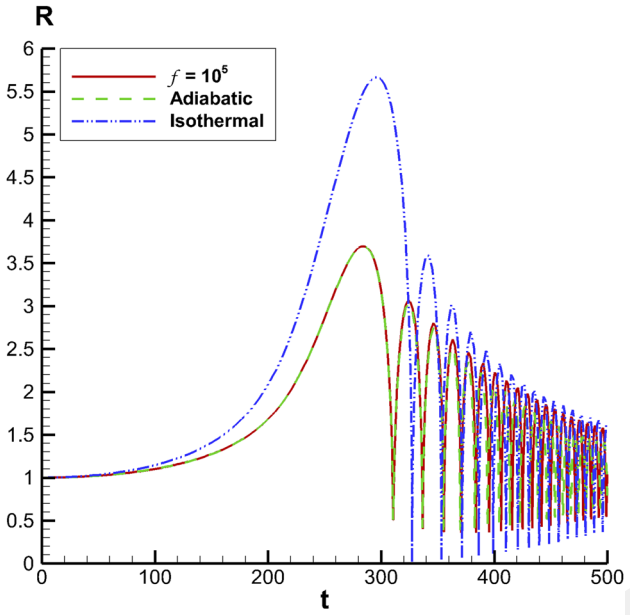


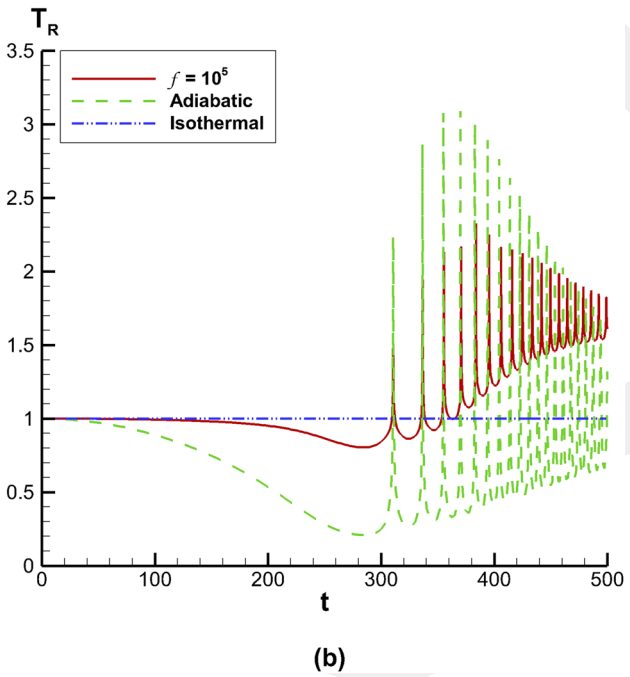


**FIG. 12.** (a) Comparison of the temporal evolution of the normalized bubble radius of the air–water vapor bubble in water under the conditions stated in Fig. 10 between results obtained by the Keller–Miksis equation (33) using the adiabatic gas law, the proposed acoustic model for $f = 10^5$, and the isothermal law. (b) Comparison of the temporal evolution of the bubble wall temperature of the air–water vapor bubble in water under the conditions stated in Fig. 10 between results obtained by the Keller–Miksis equation (33) using the adiabatic gas law, the proposed acoustic model for $f = 10^5$, and the isothermal law.

## VII. CONCLUSIONS

The energy balance equations between a spherical gas bubble and its surrounding liquid are considered in the uniform pressure approximation by an iterative scheme, which leads to hierarchy equations for the radial partial derivatives of the temperature at the bubble wall. A closure relation, based on the ansatz that approximates the complex change of state during collapse by time averaging over a characteristic time, is introduced for these hierarchy equations. Consequently, a reduced order gas pressure law, which shows a power law dependence on the bubble radius and on the bubble wall temperature, is derived where the power indices depend on the isentropic exponent of the gas and on a parameter characterizing the effects of the Péclet number and the characteristic time scale. It is shown that the isothermal and adiabatic pressure–radius relations are recovered in the appropriate limits of the parameter. A simplified version of the reduced gas pressure law where the bubble wall temperature is approximated by the bulk liquid temperature is also discussed. In particular, for small amplitude of oscillations of a gas bubble, the parameter that enters the novel gas pressure law is identified as a function of the Péclet number from the well-known linear theory. For large amplitude oscillations of the gas, the novel gas pressure law is first validated against the near-isothermal solution of Prosperetti and against the consistent near isothermal solution presented in Appendix B. Numerical simulations of the original energy equations for constant wall temperature are carried out by spectral methods, and the results obtained are verified against those that employ the novel reduced order gas pressure law for an appropriate value of the parameter. An acoustic cavitation model, based on this novel reduced order gas pressure law together with the Plesset–Zwick solution for the bubble wall temperature and the Keller–Miksis equation for spherical bubble dynamics, is then constructed. The results obtained for the temporal variations of the bubble radius and the bubble wall temperature using different acoustic pressure signals and variable interface properties show thermal behavior that lies between the classical adiabatic and isothermal change of state.

Although the acoustic model parameter, which depends on the Péclet number based on a characteristic time scale, can be approximated by its value obtained from the linear theory for low Péclet numbers (the near isothermal approximation), it seems to deviate considerably from the value obtained by the linear theory for intermediate Péclet numbers. Therefore, accurate values of the acoustic model parameter should be estimated by constructing empirical correlations of the model parameter as a function of Péclet number based on different characteristic time scales. For a complete description, the mass diffusion of the gas and vapor inside the bubble and of the gas and vapor into the liquid should also be taken into account in a similar manner. These are beyond the scope of this work and are left for future studies. A simplified version of the novel gas pressure law can then be used in the algorithms of bubbly cavitating flows.

## ACKNOWLEDGMENTS

This paper is, in part, supported by TÜBİTAK (The Scientific and Technological Research Council of Turkey) under Grant No. 117M072. Computing resources used in this work were provided by the National Center for High Performance Computing of Turkey

(UHeM) under Grant No. 1006552019. C.F.D. is grateful to Professor Andrea Prosperetti, Professor Christopher E. Brennen, and Professor Tim Colonius for valuable discussions during the 10th International Cavitation Symposium (CAV2018) in Baltimore.

## AUTHOR DECLARATIONS

### Conflict of Interest

The authors have no conflicts to disclose.

## DATA AVAILABILITY

The data that support the findings of this study are available from the corresponding author upon reasonable request.

## APPENDIX A: MODIFIED ENERGY BALANCE EQUATIONS FOR AN ACOUSTIC CAVITATION BUBBLE

With the modeling of the vapor mass transfer across the interface given in Sec. IV, we can modify the energy balance equations (1) and (3) for a single acoustic cavitation bubble. If we assume that the vapor and gas within the bubble are perfect gases with fixed vapor concentration $\mathcal{C}_0$ so that the vapor mass transfer into or out of the bubble is small enough to cause any noticeable change in the gas–vapor composition, the energy balance equations (1) and (3) take the form[31]

$$\frac{p_b}{T}\left\{\frac{\partial T}{\partial t}+\frac{1}{(Pe)\,p_b\,R^2}\left[\lambda_b(T)\,\frac{\partial T}{\partial y}-y\,\frac{\partial T}{\partial y}\bigg|_{y=1^-}-(Pe)\,\mathcal{C}_0\,y\,p_b\,R\,\frac{dR}{dt}\right]\frac{\partial T}{\partial y}\right\}=\frac{(\gamma_b-1)}{\gamma_b}\,\frac{dp_b}{dt}+\frac{1}{(Pe)\,R^2\,y^2}\,\frac{\partial}{\partial y}\left[y^2\,\lambda_b(T)\,\frac{\partial T}{\partial y}\right] \tag{A1}$$

and

$$\frac{dp_b}{dt}=\frac{3\,\gamma_b}{R}\left[\frac{1}{(Pe)\,R}\,\frac{\partial T}{\partial y}\bigg|_{y=1^-}-(1-\mathcal{C}_0)\,p_b\,\frac{dR}{dt}\right], \tag{A2}$$

where $p_b$ is the normalized total pressure of the vapor–gas mixture, $\mathcal{C}_0$ is the fixed mass concentration of the vapor given by

$$\mathcal{C}_0=\frac{\rho_v'}{\rho_b'}=\text{constant}, \tag{A3}$$

with $\rho_v'$ and $\rho_b'$, respectively, denoting the density of the vapor and the density of the vapor–gas mixture, and $\gamma_b$ is the isentropic exponent of the vapor–gas mixture defined by

$$\gamma_b=\frac{\mathcal{C}_0\left[\,\gamma_v\,\mathfrak{R}_v'/(\gamma_v-1)\,\right]+(1-\mathcal{C}_0)\left[\,\gamma_g\,\mathfrak{R}_g'/(\gamma_g-1)\,\right]}{\mathcal{C}_0\left[\,\mathfrak{R}_v'/(\gamma_v-1)\,\right]+(1-\mathcal{C}_0)\left[\,\mathfrak{R}_g'/(\gamma_g-1)\,\right]}, \tag{A4}$$

with $\gamma_v$, $\mathfrak{R}_v'$, and $\gamma_g$, $\mathfrak{R}_g'$ denoting the isentropic exponents and gas constants of the vapor and the gas, respectively. It should also be noted that the modified energy balance equations (A1) and (A2) would yield approximate solutions even for those cases where the vapor mass flux into or out of the bubble changes the noncondensable/vapor gas mixture composition considerably, provided that $\mathcal{C}_0$ is taken as the average value of vapor concentration over the characteristic time of interest. Using the iterative technique introduced in Sec. II, substituting Eq. (5) for the temperature field near the bubble wall into the modified energy balance equation (A1) and neglecting the temperature dependence of the thermal conductivity of the gas-vapor mixture, we arrive at

$$c(t;Pe)=\left(\frac{\partial T}{\partial y}\right)_{y=1^-}=\left\{\frac{(Pe)\,R^2}{2}\left[\frac{p_b}{T_R}\,\frac{dT_R}{dt}-\frac{(\gamma_b-1)}{\gamma_b}\,\frac{dp_b}{dt}\right]-\frac{1}{2}\left(\frac{\partial^2 T}{\partial y^2}\right)_{y=1^-}\right\}\left[1+\frac{\mathcal{C}_0}{2}\,(Pe)\,p_b\,R\,\frac{dR}{dt}\right]^{-1}. \tag{A5}$$

It is now clear that whenever

$$\mathcal{C}_0\ll\frac{2}{\max\left\{(Pe)\,p_b\,R\,\left|\frac{dR}{dt}\right|\right\}} \tag{A6}$$

during the final stages of collapse, Eq. (A5) for $c(t)$ becomes identical with Eq. (9) of a gas bubble. If we further make the ansatz of Eq. (17) for the second order partial radial derivative of the temperature at the bubble wall, we arrive at Eq. (18) for $c(t;Pe)$ with the function $f$ now depending on both $\mathcal{C}_0$, $Pe$, and the characteristic time $\vartheta$, with the gas pressure $p$ replaced by the mixture pressure $p_b$ and with the isentropic exponent of the gas $\gamma$ replaced by the isentropic exponent of the gas–vapor mixture $\gamma_b$. Equation (A2) can then be integrated to yield

$$p_b=p_{bi}\left[\frac{(T_R)^{1/2(1+f)}}{R^{1-\mathcal{C}_0}}\right]^{3\,\Gamma}, \tag{A7}$$

where the polytropic exponent $\Gamma$ is given by Eq. (20) with $\gamma$ replaced by $\gamma_b$. In particular, Eq. (A7) reduces to the reduced-order gas pressure law given by Eq. (19) whenever

$$\mathcal{C}_0\ll 1. \tag{A8}$$

## APPENDIX B: CONSISTENT NEAR ISOTHERMAL SOLUTION FOR LOW PÉCLET NUMBER

Here, we consider the consistent near isothermal solution for small Péclet numbers. Consequently, we expand the normalized pressure $p$, normalized temperature $T$, and the normalized radius $R$ in powers of Péclet number in the form

$$p=\frac{1}{R_{is}^3}\left[\,1+(Pe)p_1+(Pe)^2p_2+\cdots\right], \tag{B1}$$

$$T=1+(Pe)T_1+(Pe)^2T_2+\cdots, \tag{B2}$$

and

$$R=R_{is}+(Pe)R_1+(Pe)^2R_2+\cdots, \tag{B3}$$

where the first terms correspond to the isothermal values of the variables ($Pe \to 0$). Substituting the above perturbation expressions into the conservation of mass for a spherical gas bubble,

$$\frac{1}{pR^3} = 3\int_0^1 y^2\, T^{-1} dy, \tag{B4}$$

where the ideal gas law holds and where mass diffusion into and out of the bubble is neglected, leads to the relations

$$p_1 = 3\int_0^1 y^2\, T_1 dy - 3\frac{R_1}{R_{is}} \tag{B5}$$

and

$$p_2 = p_1^2 + 3\frac{R_1}{R_{is}}p_1 + 6\frac{R_1^2}{R_{is}^2} - 3\frac{R_2}{R_{is}} + 3\int_0^1 y^2\,(T_2 - T_1^2)\, dy. \tag{B6}$$

Substituting the perturbation expansions (B1)–(B3) into the normalized energy equation (1) and collecting terms of equal order of magnitude together lead to the $O(1)$ relation

$$\frac{1}{R_{is}^2}\left[3(\gamma-1)\left(\left(\frac{\partial T_1}{\partial y}\right)_R - \frac{\dot{R}_{is}}{R_{is}^2}\right) + \nabla^2 T_1\right] = 0 \tag{B7}$$

and to the $O(Pe)$ relation

$$\begin{aligned}\frac{1}{R_{is}^3}&\left\{\frac{\partial T_1}{\partial t} + R_{is}^2\left[\frac{\partial T_1}{\partial y} - y\left(\frac{\partial T_1}{\partial y}\right)_R\right]\frac{\partial T_1}{\partial y}\right\}\\ &= \frac{3(\gamma-1)}{R_{is}^2}\left\{\left(\frac{\partial T_2}{\partial y}\right)_R - 2\frac{R_1}{R_{is}}\left(\frac{\partial T_1}{\partial y}\right)_R + \frac{R_1\dot{R}_{is}}{R_{is}^3} - \frac{\dot{R}_1 + p_1\dot{R}_{is}}{R_{is}^2}\right\}\\ &\quad + \frac{1}{R_{is}^2}\left[\nabla^2 T_2 - 2\frac{R_1}{R_{is}}\nabla^2 T_1\right],\end{aligned} \tag{B8}$$

where $\nabla^2 = \frac{1}{y^2}\frac{\partial}{\partial y}\left(y^2\frac{\partial}{\partial y}\right)$ and the subscript $R$ denotes quantities evaluated at the bubble wall $y = 1^-$.

By integrating Eq. (B7) once and taking the limit $y \to 1^-$ lead to the relation

$$\left(\frac{\partial T_1}{\partial y}\right)_R = \left(\frac{\partial T_1}{\partial y}\right)_{y=1^-} = \frac{(\gamma-1)}{\gamma}\frac{\dot{R}_{is}}{R_{is}^2}. \tag{B9}$$

Furthermore, integration of Eq. (B7) using Eq. (B9) together with the condition $T_1(t,1) = 0$ yields the solution

$$T_1(t,y) = \frac{(\gamma-1)}{2\gamma}\frac{\dot{R}_{is}}{R_{is}}(y^2 - 1) \tag{B10}$$

for the first order near isothermal temperature correction $T_1(t,y)$. The first order uniform gas pressure correction $p_1(t)$ is obtained by substituting Eq. (B9) into Eq. (B5) and by carrying out the integral as

$$p_1(t) = -\frac{(\gamma-1)}{5\gamma}\frac{\dot{R}_{is}}{R_{is}} - 3\frac{R_1}{R_{is}}. \tag{B11}$$

We now carry out the near isothermal perturbation expansion of the normalized pressure equation (3). By substituting the perturbation expansions (B1)–(B3) into Eq. (3), the $O(1)$ terms cancel on both sides of the equation using Eq. (B9). The $O(Pe)$ magnitude terms lead to the relation

$$\begin{aligned}\frac{1}{R_{is}^3}&\left(\frac{dp_1}{dt} - \frac{3\dot{R}_{is}}{R_{is}}p_1\right) = \frac{3\gamma}{R_{is}^2}\left[\left(\frac{\partial T_2}{\partial y}\right)_R - 2\frac{R_1}{R_{is}}\left(\frac{\partial T_1}{\partial y}\right)_R\right.\\ &\left. + \frac{R_1\dot{R}_{is}}{R_{is}^3} - \frac{\left(\dot{R}_1 + p_1\dot{R}_{is}\right)}{R_{is}^2}\right].\end{aligned} \tag{B12}$$

If we now substitute Eq. (B11) for $p_1$ and Eq. (B9) for $(\partial T_1/\partial y)_{y=1}$, we obtain the relation

$$\begin{aligned}\left(\frac{\partial T_2}{\partial y}\right)_R &= \left(\frac{\partial T_2}{\partial y}\right)_{y=1}\\ &= -\frac{(\gamma-1)}{15\gamma^2 R_{is}^4}\left[R_{is}\ddot{R}_{is} - (5-3\gamma)\dot{R}_{is}^2\right]\\ &\quad + \frac{(\gamma-1)}{\gamma}\frac{\dot{R}_1}{R_{is}^2} - \frac{2(\gamma-1)}{\gamma}\frac{R_1\dot{R}_{is}}{R_{is}^3}.\end{aligned} \tag{B13}$$

The second order perturbation term $T_2(t,y)$ can now be obtained from Eq. (B8) using Eq. (B13) together with the condition $T_2(t,1) = 0$, which, in turn, would lead to the solution of second order perturbation pressure $p_2(t)$ by substitution. However, due to its limited use and cumbersome calculations, we herein restrict our near isothermal solution only to first order perturbations.

Finally, we consider the Keller–Miksis equation (33) in the near isothermal approximation as

$$\begin{aligned}&\left[1 - M\dot{R} + \frac{4M}{(\mathrm{Re})R}\right]R\ddot{R} + \frac{3}{2}\left[1 - \frac{M}{3}\dot{R} - \frac{8M}{3\,(\mathrm{Re})\,R}\right]\dot{R}^2\\ &\quad + \left[\frac{4(1+M\dot{R})}{(\mathrm{Re})} - \frac{2M}{(We)}\right]\frac{\dot{R}}{R} + \frac{2\,(1+M\dot{R})}{(We)}\\ &\quad \times\left[\frac{1}{R} - \frac{1}{R_{is}^3}(1 + (Pe)p_1)\right] + \frac{\sigma(1+M\dot{R})}{2}\\ &\quad \times\left[1 - \frac{1}{R_{is}^3}(1 + (Pe)p_1)\right] + \frac{(1+M\dot{R})}{2}C_p + \frac{MR}{2}\frac{dC_p}{dt}\\ &\quad - \left(\frac{2}{We} + \frac{\sigma}{2}\right)MR\,\frac{d}{dt}\left[\frac{1}{R_{is}^3}(1 + (Pe)p_1)\right] = 0,\end{aligned} \tag{B14}$$

where the cavitation number $\sigma = \sigma(1)$, the Reynolds number $Re = \mathrm{Re}(1)$, and the Weber number $We = We(1)$ are all evaluated at the isothermal temperature. By substituting the near isothermal perturbation expansions (B1)–(B3) into the above equation, the $O(1)$ terms yield the nonlinear bubble dynamics equation

$$\begin{aligned}&\left(1 - M\dot{R}_{is} + \frac{4M}{(\mathrm{Re})R_{is}}\right)R_{is}\ddot{R}_{is} + \frac{3}{2}\left(1 - \frac{M}{3}\dot{R}_{is} - \frac{8M}{3(\mathrm{Re})R_{is}}\right)\dot{R}_{is}^2\\ &\quad + \left[\frac{4(1+M\dot{R}_{is})}{(\mathrm{Re})} - \frac{2M}{(We)}\right]\frac{\dot{R}_{is}}{R_{is}} + \frac{2\,(1+M\dot{R}_{is})}{(We)}\left(\frac{1}{R_{is}} - \frac{1}{R_{is}^3}\right)\\ &\quad + \frac{\sigma(1+M\dot{R}_{is})}{2}\left(1 - \frac{1}{R_{is}^3}\right) + \frac{(1+M\dot{R}_{is})}{2}C_p + \frac{MR_{is}}{2}\frac{dC_p}{dt}\\ &\quad + 3M\left(\frac{2}{We} + \frac{\sigma}{2}\right)\frac{\dot{R}_{is}}{R_{is}^3} = 0\end{aligned} \tag{B15}$$

for $R_{is}$ and the linear bubble dynamics equation

$$\left[1 - M\dot{R}_{is} + \frac{4M}{(\mathrm{Re})R_{is}}\right]R_{is}\ddot{R}_1 + \left[3\left(1 - \frac{M}{2}\dot{R}_{is}\right)\dot{R}_{is} - MR_{is}\ddot{R}_{is} + \frac{4}{(\mathrm{Re})R_{is}} + \frac{2M}{R_{is}^3}\left(\frac{2}{We} + \frac{\sigma}{2}\right) + \frac{\sigma M}{2} + \frac{MC_p}{2}\right]\dot{R}_1 + \left[(1 - M\dot{R}_{is})\ddot{R}_{is} - \frac{4\dot{R}_{is}}{(\mathrm{Re})R_{is}^2} - \frac{2}{(We)R_{is}^2} + \frac{3(1 - 2M\dot{R}_{is})}{R_{is}^4} \times \left(\frac{2}{We} + \frac{\sigma}{2}\right) + \frac{M\dot{C}_p}{2}\right]R_1 + \left(\frac{2}{We} + \frac{\sigma}{2}\right)\frac{(\gamma - 1)}{5\gamma R_{is}^5} \times \left[\dot{R}_{is} + M(R_{is}\ddot{R}_{is} - 4\dot{R}_{is}^2)\right] = 0 \tag{B16}$$

for the perturbation radius $R_1$. The initial value problems for the isothermal bubble dynamics equation (B15) and the initial value problem for the dynamics of the perturbation bubble radius $R_1$ can be solved using the initial conditions $R_{is}(0) = 1$; $\dot{R}_{is}(0) = 0$ and $R_1(0) = 0$; $\dot{R}_1(0) = 0$, respectively.

## APPENDIX C: TEMPERATURE DEPENDENCE OF THE THERMOPHYSICAL PROPERTIES OF WATER AND WATER VAPOR

In the proposed acoustic cavitation model, the properties of the condensable liquid and vapor phases as well as those of the noncondensable gas at the interface may change considerably especially during the collapse of the bubbles due to large temperature and pressure variations at the bubble wall and in the bubble interior. Some of these properties are due to phase change (evaporation and condensation) that enter the Plesset–Zwick equation (31) in our acoustic cavitation model. These are mainly the normalized latent heat of condensation $L(T)$, the normalized saturation vapor pressure $p_{v,sat}(T)$, the normalized saturation vapor density $\rho_{v,sat}(T)$, and the normalized liquid thermal conductivity $\lambda_\ell(T)$. The normalized latent heat $L(T_R)$ is given by the Watson relation[40]

$$L(T_R) = \frac{L'(T'_R)}{L'_0} = \left(\frac{T_c - T_R}{T_c - 1}\right)^{0.375} \tag{C1}$$

for $T_R < T_c$, where $T_c = T'_c/T'_0$ is the normalized critical temperature with $T'_c$ denoting its actual value. For $T_R \geq T_c$, $L(T_R) = 0$ since there is no first order phase transition above the critical point. The normalized saturated vapor pressure $p_{v,sat}(T_R)$ is given by[40]

$$\ln\left(\frac{p_{v,sat}(T_R)}{p_c}\right) = \ln\left(\frac{p'_{v,sat}(T'_R)}{p'_c}\right) = \frac{A_v\, x + B_v\, x^{1.5} + C_v\, x^3 + D_v\, x^6}{1 - x}, \tag{C2}$$

with $A_v, B_v, C_v, D_v$ denoting fluid dependent constants and $x$ given by

$$x = 1 - \frac{T_R}{T_c} \tag{C3}$$

for $T_R < T_c$, where $p_c = p'_c/p'_0$ is the normalized critical pressure, with $p'_c$ denoting the actual value of the critical pressure and $p'_0$ denoting the initial pressure of the liquid. For water/water–vapor phase change, we have $A_v = -7.764\,51$, $B_v = 1.458\,38$, $C_v = -2.775\,80$, and $D_v = -1.233\,03$. The critical temperature of water is taken to be 647.27 K. Above the critical point $T_R \geq T_c$, the two phases (gas and vapor) cannot coexist and the Plesset–Zwick equation is no longer valid. In this case, the change of state of the gas can be taken to be adiabatic. The normalized saturated vapor density $\rho_{v,sat}(T_R)$ can then be approximately obtained using the ideal gas law for the vapor phase,

$$\rho_{v,sat}(T_R) = \frac{\rho'_{v,sat}(T'_R)}{\rho'_{v0,sat}} = \frac{p_{v,sat}(T_R)}{T_R\, p_{v,sat}(1)}, \tag{C4}$$

where $p_{v,sat}(T_R)$ is obtained from Eq. (C2) above and $T_R$ is given by the Plesset–Zwick solution whenever $T_R < T_c$. A more accurate prediction for the normalized saturated vapor density can be obtained using the virial equation of state for the vapor. In this case, the normalized saturated vapor pressure is given by

$$\rho_{v,sat}(T_R) = \frac{p_{v,sat}(T_R)}{T_R\, p_{v,sat}(1)} \frac{\left[1 - \left(B'_0\, p'_{v0,sat}/M'\, \Re'_v\, T'_0\right)\left(B(T_R)p_{v,sat}(T_R)/T_R\, p_{v,sat}(1)\right)\right]}{\left[1 - \left(B'_0\, p'_{v0,sat}/M'\, \Re'_v\, T'_0\right)\right]}, \tag{C5}$$

where $M'$ is the molecular weight of the vapor (for water vapor $M' = 18.015 \times 10^{-3}$ kg mol). In Eq. (C5), $B(T_R)$ is the normalized second virial coefficient at the bubble wall temperature given by[41]

$$B(T_R) = a_1\, T_R^{*-0.5} + a_2\, T_R^{*-0.8} + a_3\, T_R^{*-3.35} + a_4\, T_R^{*-8.3}, \tag{C6}$$

with $a_1, a_2, a_3, a_4$ denoting fluid dependent constants, $T_R^* = T'_R/T'_c$ and with $B'_0$ denoting the value of the second virial coefficient at the cold liquid temperature (for water vapor, $a_1 = 0.344\,04$, $a_2 = -0.758\,26$, $a_3 = -24.219$, $a_4 = -3978.2$, and $B'_0 = 0.001$ mol$^{-1}$). Other thermophysical properties at the interface include the surface tension $S'(T'_R)$ that enters the Weber number, the liquid viscosity $\mu'_\ell(T'_R)$ that enters the Reynolds number, and the thermal conductivity of the liquid $\lambda'_\ell(T'_R)$ that enters the Plesset–Zwick law. The variation of the surface tension $S'(T'_R)$ is given universally by[40]

$$S'(T'_R) = S'_0\left(\frac{T_c - T_R}{T_c - 1}\right)^{4n} \tag{C7}$$

for $T_R < T_c$, where $n$ is between 0.25 and 0.31 (the corresponding state value is $n = 0.305$) and $S'_0$ is the value of the surface tension at the cold liquid temperature. The temperature dependence of the viscosity of the liquid is given by the relation[40]

$$\ln\left(\frac{\mu'(T'_R)}{\mu'_r}\right) = a + b\left(\frac{T'_r}{T'_R}\right) + c\left(\frac{T'_r}{T'_R}\right)^2, \tag{C8}$$

where $a$, $b$, and $c$ are liquid dependent constants, $T'_r$ is some reference temperature, and $\mu'_r$ is the liquid viscosity at that temperature (for liquid water, $a = -1.94$, $b = -480.0$, $c = 6.74$, $T'_r = 273.16$ K, and $\mu'_r = 0.001\,792$ kg/m s). Finally, the thermal conductivity of the liquid may be taken to be quadratic,[40]

$$\lambda'_\ell(T'_R) = A + B\,T'_R + C\,T'^2_R. \tag{C9}$$

For liquid water $A = -0.3838$ W/m K, $B = 5.254 \times 10^{-3}$ W/m K$^2$, and $C = -6.369 \times 10^{-6}$ W/m K$^3$.

## REFERENCES


[1] C. E. Brennen, *Cavitation and Bubble Dynamics* (Oxford University Press, Oxford, 1995), pp. 37–43.
[2] M. S. Plesset and A. Prosperetti, "Bubble dynamics and cavitation," Annu. Rev. Fluid Mech. **9**, 145 (1977).
[3] T. G. Leighton, *The Acoustic Bubble* (Academic Press, London, 1994), pp. 287–379.
[4] K. S. Suslick, "Sonochemistry," Science **247**, 1439 (1990).
[5] D. F. Gaitan, L. A. Crum, C. C. Church, and R. A. Roy, "Sonoluminescence and bubble dynamics for a single, stable, cavitation bubble," J. Acoust. Soc. Am. **91**(6), 3166 (1992).
[6] L. A. Crum, "Sonoluminescence," Phys. Today **47**(9), 22 (1994).
[7] K. Ferrara, R. Pollard, and M. Borden, "Ultrasound microbubble contrast agents: Fundamentals and application to gene and drug delivery," Annu. Rev. Biomed. Eng. **9**, 415 (2007).
[8] S. Qin, C. F. Caskey, and K. W. Ferrara, "Ultrasound contrast microbubbles in imaging and therapy: Physical principles and engineering," Phys. Med. Biol. **54**(6), R27 (2009).
[9] R. I. Nigmatulin, N. S. Khabeev, and F. B. Nagiev, "Dynamics, heat and mass transfer of vapour-gas bubbles in a liquid," Int. J. Heat Mass Transfer **24**(6), 1033 (1981).
[10] Y. Matsumoto and F. Takemura, "Influence of internal phenomena on gas bubble motion," JSME Int. J., Ser. B **37**(2), 288 (1994).
[11] A. Prosperetti, L. A. Crum, and K. W. Commander, "Nonlinear bubble dynamics," J. Acoust. Soc. Am. **83**(2), 502 (1988).
[12] A. Prosperetti, "The thermal behavior of oscillating gas bubbles," J. Fluid Mech. **222**, 587 (1991).
[13] R. Toegel, B. Gompf, R. Pecha, and D. Lohse, "Does water vapor prevent upscaling sonoluminescence?," Phys. Rev. Lett. **85**(15), 3165 (2000).
[14] A. T. Preston, T. Colonius, and C. E. Brennen, "A reduced-order model of diffusive effects on the dynamics of bubbles," Phys. Fluids **19**, 123302 (2007).
[15] L. Stricker, A. Prosperetti, and D. Lohse, "Validation of an approximate model for the thermal behavior in acoustically driven bubbles," J. Acoust. Soc. Am. **130**(5), 3243 (2011).
[16] W. Kreider, L. A. Crum, M. R. Bailey, and O. A. Sapozhnikov, "A reduced-order, single-bubble cavitation model with applications to therapeutic ultrasound," J. Acoust. Soc. Am. **130**(5), 3511 (2011).
[17] Y. A. Gadi Man and F. J. Trujillo, "A new pressure formulation for gas-compressibility dampening in bubble dynamics models," Ultrason. Sonochem. **32**, 247 (2016).
[18] L. Bergamasco and D. Fuster, "Oscillation regimes of gas/vapor bubbles," Int. J. Heat Mass Transfer **112**, 72 (2017).
[19] X. Zhong, J. Eshraghi, P. Vlachos, S. Dabiri, and A. M. Ardekani, "A model for a laser-induced cavitation bubble," Int. J. Multiphase Flow **132**, 103433 (2020).
[20] T. Kanagawa and T. Kamei, "Thermal effect inside bubbles for weakly nonlinear pressure waves in bubbly liquids: Theory on short waves," Phys. Fluids **33**, 063319 (2021).
[21] C. F. Delale and Ş. Pasinlioğlu, "First iterative solution of the thermal behavior of acoustic cavitation bubbles in the uniform pressure approximation," J. Phys.: Conf. Ser. **656**, 012016 (2015).
[22] C. F. Delale and S. Pasinlioglu, "A reduced order gas pressure law for single acoustic cavitation bubbles," in *Proceedings of the 10th International Symposium on Cavitation (CAV2018)*, edited by J. Katz (ASME e-book, Baltimore, MD, 2018), CAV18-05007.
[23] M. S. Plesset and S. A. Zwick, "A nonsteady heat diffusion problem with spherical symmetry," J. Appl. Phys. **23**(1), 95 (1952).
[24] C. Devin, "Survey of thermal, radiation and viscous damping of pulsating air bubbles in water," J. Acoust. Soc. Am. **31**(12), 1654 (1959).
[25] H. Pfriem, "Zur thermischen dämpfung inkugelsymmetrisch schwingenden gasblasen," Akust. Zh. **5**, 202 (1940).
[26] A. Prosperetti, "Bubble phenomena in sound fields: Part one," Ultrasonics **22**, 69 (1984).
[27] A. I. Eller, "Damping constants of pulsating bubbles," J. Acoust. Soc. Am. **47**, 1469 (1970).
[28] A. Prosperetti, "Thermal effects and damping mechanisms in the forced radial oscillations of gas bubbles in liquids," J. Acoust. Soc. Am. **61**(1), 17 (1977).
[29] L. A. Crum, "The polytropic exponent of gas contained within air bubbles pulsating within a liquid," J. Acoust. Soc. Am. **73**, 116 (1983).
[30] J. B. Keller and M. Miksis, "Bubble oscillations of large amplitude," J. Acoust. Soc. Am. **68**, 628 (1980).
[31] C. F. Delale, "Thermal damping in cavitating nozzle flows," J. Fluids Eng. **124**(4), 969 (2002).
[32] S. Putterman, P. G. Evans, G. Vazquez, and K. Weninger, "Is there a simple theory of sonoluminescence?," Nature **409**, 782 (2001).
[33] Y. Hao and A. Prosperetti, "The dynamics of vapor bubbles inacoustic pressure fields," Phys. Fluids **11**(8), 2008 (1999).
[34] F. R. Gilmore, "The collapse and growth of a spherical bubble in a viscous compressible liquid," Hydrodynamics Laboratory Report No. 26-4, California Institute of Technology, 1952.
[35] Y. Tomita and A. Shima, "On the behavior of a spherical bubble and the impulse pressure in a viscous compressible liquid," Bull. JSME **20**, 1453 (1977).
[36] A. Prosperetti and A. Lezzi, "Bubble dynamics in a compressible liquid. Part 1. First-order theory," J. Fluid Mech. **168**, 457 (1986).
[37] K. Ando, T. Sanada, K. Inaba, J. S. Damazo, J. E. Shepherd, T. Colonius, and C. E. Brennen, "Shock propagation through a bubbly liquid in a deformable tube," J. Fluid Mech. **671**, 339 (2011).
[38] A. T. Preston, "Modeling heat and mass transfer in bubbly cavitating flows and shock waves in cavitating nozzles," Ph.D. thesis, California Institute of Technology, 2004.
[39] Y. Wang, "Shock waves in bubbly cavitating flows," Ph.D. thesis, California Institute of Technology, 1996.
[40] R. M. Reid, J. M. Prausnitz, and B. E. Poling, *The Properties of Gases and Liquids* (McGraw-Hill, New York, 1987).
[41] A. H. Harvey and E. W. Lemmon, "Correlation for the second virial coefficient of water," J. Phys. Chem. Ref. Data **33**(1), 369 (2004).